



HAL
open science

A Wasserstein-type distance in the space of Gaussian Mixture Models

Julie Delon, Agnès Desolneux

► **To cite this version:**

Julie Delon, Agnès Desolneux. A Wasserstein-type distance in the space of Gaussian Mixture Models. SIAM Journal on Imaging Sciences, 2020, 13 (2), pp.936-970. hal-02178204v1

HAL Id: hal-02178204

<https://hal.science/hal-02178204v1>

Submitted on 9 Jul 2019 (v1), last revised 9 Jun 2020 (v4)

HAL is a multi-disciplinary open access archive for the deposit and dissemination of scientific research documents, whether they are published or not. The documents may come from teaching and research institutions in France or abroad, or from public or private research centers.

L'archive ouverte pluridisciplinaire **HAL**, est destinée au dépôt et à la diffusion de documents scientifiques de niveau recherche, publiés ou non, émanant des établissements d'enseignement et de recherche français ou étrangers, des laboratoires publics ou privés.

A Wasserstein-type distance in the space of Gaussian Mixture Models*

Julie Delon[†] and Agnès Desolneux[‡]

Abstract. In this paper we introduce a Wasserstein-type distance on the set of Gaussian mixture models. This distance is defined by restricting the set of possible coupling measures in the optimal transport problem to Gaussian mixture models. We derive a very simple discrete formulation for this distance, which makes it suitable for high dimensional problems. We also study the corresponding multi-marginal and barycenter formulations. We show some properties of this Wasserstein-type distance, and we illustrate its practical use with some examples in image processing.

Key words. optimal transport, Wasserstein distance, Gaussian mixture model, multi-marginal optimal transport, barycenter, image processing applications

AMS subject classifications. 65K10, 65K05, 90C05, 62-07, 68Q25, 68U10, 68U05, 68R10

1. Introduction. Nowadays, Gaussian Mixture Models (GMM) have become ubiquitous in statistics and machine learning. These models are especially useful in applied fields to represent probability distributions of real datasets. Indeed, as linear combinations of Gaussian distributions, they are perfect to model complex multimodal densities and can approximate any continuous density when the numbers of components is chosen large enough. Their parameters are also easy to infer with algorithms such as the Expectation-Maximization (EM) algorithm [8]. For instance, in image processing, a large body of works use GMM to represent patch distributions in images¹, and use these distributions for various applications, such as image restoration [27, 20, 26, 23, 14, 7] or texture synthesis [11].

The optimal transport theory provides mathematical tools to compare or interpolate between probability distributions. For two probability distributions μ_0 and μ_1 on \mathbb{R}^d and a positive cost function c on $\mathbb{R}^d \times \mathbb{R}^d$, the goal is to solve the optimization problem

$$(1.1) \quad \inf_{Y_0 \sim \mu_0; Y_1 \sim \mu_1} \mathbb{E}(c(Y_0, Y_1)),$$

where the notation $Y \sim \mu$ means that Y is a random variable with probability distribution μ . When $c(x, y) = \|x - y\|^p$ for $p \geq 1$, Equation (1.1) (to a power $1/p$) defines a distance between probability distributions that have a moment of order p , called the Wasserstein distance W_p .

While this subject has gathered a lot of theoretical work (see [21, 22, 19] for three reference monographies on the topic), its success in applied fields was slowed down for many years by the computational complexity of numerical algorithms which were not always compatible with large amount of data. In recent years, the development of efficient numerical approaches

*Submitted to the editors DATE.

Funding: This work was funded by the French National Research Agency under the grant ANR-14-CE27-0019 - MIRIAM.

[†]MAP5, Univ. Paris Descartes, France (julie.delon@parisdescartes.fr)

[‡]CMLA, CNRS and ENS Paris-Saclay, France (agnes.desolneux@cmla.ens-cachan.fr)

¹Patches are small image pieces, they can be seen as vectors in a high dimensional space.

has been a game changer, widening the use of optimal transport to various applications notably in image processing, computer graphics and machine learning [15]. However, computing Wasserstein distances or optimal transport plans remains intractable when the dimension of the problem is too high.

Optimal transport can be used to compute distances or geodesics between Gaussian mixture models, but optimal transport plans between GMM, seen as probability distributions on a higher dimensional space, are usually not Gaussian mixture models themselves, and the corresponding Wasserstein geodesics between GMM do not preserve the property of being a GMM. In order to keep the good properties of these models, we define in this paper a variant of the Wasserstein distance by restricting the set of possible coupling measures to Gaussian mixture models. The idea of restricting the set of possible coupling measures has already been explored for instance in [3], where the distance is defined on the set of the probability distributions of strong solutions to stochastic differential equations. The goal of the authors is to define a distance which keeps the good properties of W_2 while being numerically tractable.

In this paper, we show that restricting the set of possible coupling measures to Gaussian mixture models transforms the original infinitely dimensional optimization problem into a finite dimensional problem with a simple discrete formulation, depending only on the parameters of the different Gaussian distributions in the mixture. When the ground cost is simply $c(x, y) = \|x - y\|^2$, this yields a geodesic distance, that we call GW_2 , which is obviously larger than W_2 , and is always upper bounded by W_2 plus a term depending only on the trace of the covariance matrices of the Gaussian components in the mixture. The complexity of the corresponding discrete optimization problem does not depend on the space dimension, but only on the number of components in the different mixtures, which makes it particularly suitable in practice for high dimensional problems. Observe that this equivalent discrete formulation has been proposed twice very recently in the machine learning literature, by two independent teams [5, 6]. We also study the multi-marginal and barycenter formulations of the problem, and show the link between these formulations.

The paper is organized as follows. Section 2 is a reminder on Wasserstein distances and barycenters between probability measures on \mathbb{R}^d . We also recall the explicit formulation of W_2 between Gaussian distributions. In Section 3, we recall some properties of Gaussian mixture models, focusing on an identifiability property that will be necessary for the rest of the paper. We also show that optimal transport plans for W_2 between GMM are generally not GMM themselves. Then, Section 4 introduces the GW_2 distance and derives the corresponding discrete formulation. Section 5 compares GW_2 with W_2 , and Section 6 focuses on the corresponding multi-marginal and barycenter formulations. We conclude in Section 8 with two applications of the distance GW_2 to image processing.

Notations. We define in the following some of the notations that will be used in the paper.

- The notation $Y \sim \mu$ means that Y is a random variable with probability distribution μ .
- If μ is a positive measure on a space \mathcal{X} and $T : \mathcal{X} \rightarrow \mathcal{Y}$ is an application, $T\#\mu$ stands for the push-forward measure of μ by T , *i.e.* the measure on \mathcal{Y} such that $\forall A \subset \mathcal{Y}$, $(T\#\mu)(A) = \mu(T^{-1}(A))$.
- The notation $\text{tr}(M)$ denotes the trace of the matrix M .

- The notation Id is the identity application.
- $\langle \xi, \xi' \rangle$ denotes the Euclidean scalar product between ξ and ξ' in \mathbb{R}^d .
- $\mathcal{M}_{n,m}(\mathbb{R})$ is the set of real matrices with n lines and m columns, and we denote by $\mathcal{M}_{n_0, n_1, \dots, n_{J-1}}(\mathbb{R})$ the set of J dimensional tensors of size n_k in dimension k .
- $\mathbf{1}_n = (1, 1, \dots, 1)^t$ denotes a column vector of ones of length n .
- For a given vector m in \mathbb{R}^d and a $d \times d$ covariance matrix Σ , $g_{m, \Sigma}$ denotes the density of the Gaussian (multivariate normal) distribution $\mathcal{N}(\mu, \Sigma)$.
- When a_i is a finite sequence of K elements (real numbers, vectors or matrices), we denote its elements as a_i^0, \dots, a_i^{K-1} .

2. Background: Wasserstein distances and barycenters between probability measures on \mathbb{R}^d . Let $d \geq 1$ be an integer. We recall in this section the definition and some basic properties of the Wasserstein distances between probability measures on \mathbb{R}^d . We write $\mathcal{P}(\mathbb{R}^d)$ the set probability measures on \mathbb{R}^d . For $p \geq 1$, the Wasserstein space $\mathcal{P}_p(\mathbb{R}^d)$ is defined as the set of probability measures μ with a finite moment of order p , *i.e.* such that

$$\int_{\mathbb{R}^d} \|x\|^p d\mu(x) < +\infty,$$

with $\|\cdot\|$ the Euclidean norm on \mathbb{R}^d .

For $t \in [0, 1]$, we define $P_t : \mathbb{R}^d \times \mathbb{R}^d \rightarrow \mathbb{R}^d$ by

$$\forall x, y \in \mathbb{R}^d, \quad P_t(x, y) = (1-t)x + ty \in \mathbb{R}^d.$$

Observe that P_0 and P_1 are the projections from $\mathbb{R}^d \times \mathbb{R}^d$ onto \mathbb{R}^d such that $P_0(x, y) = x$ and $P_1(x, y) = y$.

2.1. Wasserstein distances. Let $p \geq 1$, and let μ_0, μ_1 be two probability measures in $\mathcal{P}_p(\mathbb{R}^d)$. Define $\Pi(\mu_0, \mu_1) \subset \mathcal{P}_p(\mathbb{R}^d \times \mathbb{R}^d)$ as being the subset of probability distributions γ on $\mathbb{R}^d \times \mathbb{R}^d$ with marginal distributions μ_0 and μ_1 , *i.e.* such that $P_0\#\gamma = \mu_0$ and $P_1\#\gamma = \mu_1$. The p -Wasserstein distance W_p between μ_0 and μ_1 is defined as

$$(2.1) \quad W_p^p(\mu_0, \mu_1) := \inf_{Y_0 \sim \mu_0; Y_1 \sim \mu_1} \mathbb{E}(\|Y_0 - Y_1\|^p) = \inf_{\gamma \in \Pi(\mu_0, \mu_1)} \int_{\mathbb{R}^d \times \mathbb{R}^d} \|y_0 - y_1\|^p d\gamma(y_0, y_1).$$

This formulation is a special case of (1.1) when $c(x, y) = \|x - y\|^p$. It can be shown (see for instance [22]) that there is always a couple (Y_0, Y_1) of random variables which attains the infimum (hence a minimum) in the previous energy. Such a couple is called an *optimal coupling*. The probability distribution γ of this couple is called an *optimal transport plan* between μ_0 and μ_1 . This plan distributes all the mass of the distribution μ_0 onto the distribution μ_1 with a minimal cost, and the quantity $W_p^p(\mu_0, \mu_1)$ is the corresponding total cost.

As suggested by its name (p -Wasserstein distance), W_p defines a metric on $\mathcal{P}_p(\mathbb{R}^d)$. It also metrizes the weak convergence² in $\mathcal{P}_p(\mathbb{R}^d)$ (see [22], chapter 6). It follows that W_p is continuous on $\mathcal{P}_p(\mathbb{R}^d)$ for the topology of weak convergence.

From now on, we will mainly focus on the case $p = 2$, since W_2 has an explicit formulation if μ_0 and μ_1 are Gaussian measures.

²A sequence $(\mu_k)_k$ converges weakly to μ in $\mathcal{P}_p(\mathbb{R}^d)$ if it converges to μ in the sense of distributions and if $\int \|y\|^p d\mu_k(y)$ converges to $\int \|y\|^p d\mu(y)$.

2.2. Transport map and transport plan. Assume that $p = 2$. When μ_0 and μ_1 are two probability distributions on \mathbb{R}^d and assuming that μ_0 is absolutely continuous, then it can be shown that the optimal transport plan γ for the problem (2.1) is unique and has the form

$$(2.2) \quad \gamma = (\text{Id}, T) \# \mu_0,$$

where $T : \mathbb{R}^d \mapsto \mathbb{R}^d$ is an application called *optimal transport map* and satisfying $T \# \mu_0 = \mu_1$ (see [22]). It means that for A, B Borel sets of \mathbb{R}^d , if f_0 denotes the probability density of μ_0 , we have

$$\begin{aligned} \gamma(A \times B) &= \mu_0((\text{Id}, T)^{-1}(A, B)) = \mu_0(A \cap T^{-1}(B)) \\ &= \int_{A \cap T^{-1}(B)} f_0(x) dx = \int_A f_0(x) \mathbf{1}_{T^{-1}(B)}(x) dx \\ &= \int_A f_0(x) \mathbf{1}_B(T(x)) dx = \int_{A \times B} f_0(x) \delta_{y=T(x)} dx dy. \end{aligned}$$

2.3. Displacement interpolation. If γ is an optimal transport plan for W_2 between two probability distributions μ_0 and μ_1 , the path $(\mu_t)_{t \in [0,1]}$ given by

$$\forall t \in [0, 1], \quad \mu_t := P_t \# \gamma$$

defines a constant speed geodesic in $\mathcal{P}_2(\mathbb{R}^d)$ (see for instance [19] Ch.5, Section 5.4).

When there is an optimal transport map T between μ_0 and μ_1 , then we have

$$\mu_t = ((1-t)\text{Id} + tT) \# \mu_0.$$

The path $(\mu_t)_{t \in [0,1]}$ is the displacement interpolation between μ_0 and μ_1 and it satisfies the following properties:

- For all $t, s \in [0, 1]$, we have $W_2(\mu_t, \mu_s) = |t - s|W_2(\mu_0, \mu_1)$.
- The length of the path $(\mu_t)_{t \in [0,1]}$ defined by

$$\text{Len}((\mu_t)_{t \in [0,1]}) = \text{Sup}_{N; 0=t_0 \leq t_1 \dots \leq t_N=1} \sum_{i=1}^N W_2(\mu_{t_{i-1}}, \mu_{t_i}),$$

satisfies $\text{Len}((\mu_t)_{t \in [0,1]}) = W_2(\mu_0, \mu_1)$, making $(\mathcal{P}_2(\mathbb{R}^d), W_2)$ a geodesic space.

- For $t \in (0, 1)$ we also have that μ_t is a weighted barycenter of μ_0 and μ_1 , that is:

$$(2.3) \quad \mu_t \in \underset{\rho}{\text{argmin}} (1-t)W_2(\mu_0, \rho)^2 + tW_2(\mu_1, \rho)^2.$$

This notion of barycenter, often called Wasserstein barycenter in the literature, can be easily extended to more than two probability distributions, as recalled in the next paragraphs.

2.4. Multi-marginal formulation and barycenters. For $J \geq 2$, for a set of weights $\lambda = (\lambda_0, \dots, \lambda_{J-1}) \in (\mathbb{R}_+)^J$ such that $\lambda \mathbf{1}_J = \lambda_0 + \dots + \lambda_{J-1} = 1$ and for $x = (x_0, \dots, x_{J-1}) \in (\mathbb{R}^d)^J$, we write

$$(2.4) \quad B(x) = \sum_{i=0}^{J-1} \lambda_i x_i = \underset{y \in \mathbb{R}^d}{\text{argmin}} \sum_{i=0}^{J-1} \lambda_i \|x_i - y\|^2$$

the barycenter of the x_i with weights λ_i .

For J probability distributions $\mu_0, \mu_1, \dots, \mu_{J-1}$ on \mathbb{R}^d , we say that ν^* is the barycenter of the μ_j with weights λ_j if ν^* is solution of

$$(2.5) \quad \inf_{\nu \in \mathcal{P}_2(\mathbb{R}^d)} \sum_{j=0}^{J-1} \lambda_j W_2^2(\mu_j, \nu).$$

Existence and unicity of barycenters for W_2 has been studied in depth by Agueh and Carlier in [1]. They show in particular that if one of the μ_j has a density, this barycenter is unique. They also show that the solutions of the barycenter problem are related to the solutions of the multi-marginal transport problem (studied by Gangbo and Świąch in [12])

$$(2.6) \quad \begin{aligned} MW_2(\mu_0, \dots, \mu_{J-1}) &:= \inf_{Y_0 \sim \mu_0, \dots, Y_{J-1} \sim \mu_{J-1}} \mathbb{E} \left(\frac{1}{2} \sum_{i,j=0}^{J-1} \lambda_i \lambda_j \|Y_i - Y_j\|^2 \right), \\ &= \inf_{\gamma \in \Pi(\mu_0, \mu_1, \dots, \mu_{J-1})} \int_{\mathbb{R}^d \times \dots \times \mathbb{R}^d} \frac{1}{2} \sum_{i,j=0}^{J-1} \lambda_i \lambda_j \|y_i - y_j\|^2 d\gamma(y_0, y_1, \dots, y_{J-1}), \end{aligned}$$

where $\Pi(\mu_0, \mu_1, \dots, \mu_{J-1})$ is the set of probability measures on $(\mathbb{R}^d)^J$ having $\mu_0, \mu_1, \dots, \mu_{J-1}$ as marginals. More precisely, they show that if (2.6) has a solution γ^* , then $\nu^* = B\#\gamma^*$ is a solution of (2.5), and the infimum of (2.6) and (2.5) are equal, *i.e.*

$$(2.7) \quad MW_2(\mu_0, \dots, \mu_{J-1}) = \inf_{\nu \in \mathcal{P}_2(\mathbb{R}^d)} \sum_{j=0}^{J-1} \lambda_j W_2^2(\mu_j, \nu).$$

2.5. Optimal transport between Gaussian distributions. Computing optimal transport plans between probability distributions is usually difficult. In some specific cases, an explicit solution is known. For instance, in the one dimensional ($d = 1$) case, when the cost c is a convex function of the Euclidean distance on the line, the optimal plan consists in a monotone rearrangement of the distribution μ_0 into the distribution μ_1 (the mass is transported monotonically from left to right, see for instance Ch.2, Section 2.2 of [21] for all the details). Another case where the solution is known for a quadratic cost is the Gaussian case in any dimension $d \geq 1$.

2.5.1. Distance W_2 between Gaussian distributions. If $\mu_i = \mathcal{N}(m_i, \Sigma_i)$, $i \in \{0, 1\}$ are two Gaussian distributions on \mathbb{R}^d , the 2-Wasserstein distance W_2 between μ_0 and μ_1 has a closed-form expression, which can be written

$$(2.8) \quad W_2^2(\mu_0, \mu_1) = \|m_0 - m_1\|^2 + \text{tr} \left(\Sigma_0 + \Sigma_1 - 2 \left(\Sigma_0^{\frac{1}{2}} \Sigma_1 \Sigma_0^{\frac{1}{2}} \right)^{\frac{1}{2}} \right),$$

where, for every symmetric semi-definite positive matrix M , the matrix $M^{\frac{1}{2}}$ is its unique semi-definite positive square root.

If Σ_0 is non-singular, then the optimal map T between μ_0 and μ_1 turns out to be affine and is given by

$$(2.9) \quad \forall x \in \mathbb{R}^d, \quad T(x) = m_1 + \Sigma_0^{-\frac{1}{2}} \left(\Sigma_0^{\frac{1}{2}} \Sigma_1 \Sigma_0^{\frac{1}{2}} \right)^{\frac{1}{2}} \Sigma_0^{-\frac{1}{2}} (x - m_0) = m_1 + \Sigma_0^{-1} (\Sigma_0 \Sigma_1)^{\frac{1}{2}} (x - m_0),$$

and the optimal plan γ is then a Gaussian distribution on $\mathbb{R}^d \times \mathbb{R}^d = \mathbb{R}^{2d}$ that is degenerate since it is supported by the affine line $y = T(x)$. These results have been known since [9].

Moreover, if Σ_0 and Σ_1 are non-degenerate, the geodesic path (μ_t) , $t \in (0, 1)$, between μ_0 and μ_1 is given by $\mu_t = \mathcal{N}(m_t, \Sigma_t)$ with $m_t = (1 - t)m_0 + tm_1$ and

$$\Sigma_t = ((1 - t)\mathbf{I}_d + tC)\Sigma_0((1 - t)\mathbf{I}_d + tC),$$

with \mathbf{I}_d the $d \times d$ identity matrix and $C = \Sigma_1^{\frac{1}{2}} \left(\Sigma_1^{\frac{1}{2}} \Sigma_0 \Sigma_1^{\frac{1}{2}} \right)^{-\frac{1}{2}} \Sigma_1^{\frac{1}{2}}$.

This property still holds if the covariance matrices are not invertible, by replacing the inverse by the Moore-Penrose pseudo-inverse matrix, see Proposition 6.1 in [24]. The optimal map T is not generalized in this case since the optimal plan is usually not supported by the graph of a function.

2.5.2. W_2 -Barycenters in the Gaussian case. For $J \geq 2$, let $\lambda = (\lambda_0, \dots, \lambda_{J-1}) \in (\mathbb{R}_+)^J$ be a set of positive weights summing to 1 and let $\mu_0, \mu_1, \dots, \mu_{J-1}$ be J Gaussian probability distributions on \mathbb{R}^d . For $j = 0 \dots J - 1$, we denote by m_j and Σ_j the expectation and the covariance matrix of μ_j . Theorem 2.2 in [18] tells us that if the covariances Σ_j are all positive definite, then the solution of the multi-marginal problem (2.6) for the Gaussian distributions $\mu_0, \mu_1, \dots, \mu_{J-1}$ can be written

$$(2.10) \quad \gamma^*(x_0, \dots, x_{J-1}) = g_{m_0, \Sigma_0}(x_0) \delta_{(x_1, \dots, x_{J-1}) = (S_1 S_0^{-1} x_0, \dots, S_{J-1} S_0^{-1} x_0)}$$

where $S_j = \Sigma_j^{1/2} \left(\Sigma_j^{1/2} \Sigma_* \Sigma_j^{1/2} \right)^{-1/2} \Sigma_j^{1/2}$ with Σ_* a solution of the fixed-point problem

$$(2.11) \quad \sum_{j=0}^{J-1} \lambda_j \left(\Sigma_*^{1/2} \Sigma_j \Sigma_*^{1/2} \right)^{1/2} = \Sigma_*.$$

The barycenter ν^* of all the μ_j with weights λ_j is the distribution $\mathcal{N}(m_*, \Sigma_*)$, with $m_* = \sum_{j=0}^{J-1} \lambda_j m_j$. Equation (2.11) provides a natural iterative algorithm (see [2]) to compute the fixed point Σ_* from the set of covariances Σ_j , $j \in \{0, \dots, J - 1\}$.

3. Some properties of Gaussian Mixtures Models. The goal of this paper is to investigate how the optimisation problem (2.1) is transformed when the probability distributions μ_0, μ_1 are finite Gaussian mixture models and the transport plan γ is forced to be a Gaussian mixture model. This will be the aim of Section 4. Before, we first need to recall a few basic properties on these mixture models, and especially a density property and an identifiability property.

In the following, for $N \geq 1$ integer, we define the simplex $\Gamma_N = \{\pi \in \mathbb{R}_+^N ; \pi \mathbf{1}_N = \sum_{k=1}^N \pi_k = 1\}$.

Definition 1. Let $K \geq 1$ be an integer. A (finite) Gaussian mixture model of size K on \mathbb{R}^d is a probability distribution μ on \mathbb{R}^d that can be written

$$(3.1) \quad \mu = \sum_{k=1}^K \pi_k \mu_k \quad \text{where } \mu_k = \mathcal{N}(m_k, \Sigma_k) \text{ and } \pi \in \Gamma_K.$$

We write $GMM_d(K)$ the subset of $\mathcal{P}(\mathbb{R}^d)$ made of probability measures on \mathbb{R}^d which can be written as Gaussian mixtures with less than K components (such mixtures are obviously also in $\mathcal{P}_p(\mathbb{R}^d)$ for any $p \geq 1$). For $K < K'$, $GMM_d(K) \subset GMM_d(K')$. The set of all finite Gaussian mixture distributions is written

$$GMM_d(\infty) = \cup_{K \geq 0} GMM_d(K).$$

3.1. Density of $GMM_d(\infty)$ in $\mathcal{P}_p(\mathbb{R}^d)$. The following lemma states that any measure in $\mathcal{P}_p(\mathbb{R}^d)$ can be approximated with any precision for the distance W_p by a finite convex combination of Dirac masses. This result will be useful in the rest of the paper.

Lemma 3.1. *The set*

$$\left\{ \sum_{k=1}^N \pi_k \delta_{y_k} ; N \in \mathbb{N}, (y_k)_k \in (\mathbb{R}^d)^N, (\pi_k)_k \in \Gamma_N \right\}$$

is dense in $\mathcal{P}_p(\mathbb{R}^d)$ for the metric W_p , for any $p \geq 1$.

Proof. The proof is adapted from the proof of Theorem 6.18 in [22] and given here for the sake of completeness.

Let $\mu \in \mathcal{P}_p(\mathbb{R}^d)$. For each $\epsilon > 0$, we can find r such that $\int_{B(0,r)^c} \|y\|^p d\mu(x) \leq \epsilon^p$, where $B(0,r) \subset \mathbb{R}^d$ is the ball of center 0 and radius r , and $B(0,r)^c$ denotes its complementary set in \mathbb{R}^d . The ball $B(0,r)$ can be covered by a finite number of balls $B(y_k, \epsilon)$, $1 \leq k \leq N$. Now, define $B_k = B(y_k, \epsilon) \setminus \cup_{1 \leq j < k} B(y_j, \epsilon)$, all these sets are disjoint and still cover $B(0,r)$. Define $\phi : \mathbb{R}^d \rightarrow \mathbb{R}^d$ on \mathbb{R}^d such that

$$\forall y \in B_k \cap B(0,r), \phi(y) = y_k \quad \text{and} \quad \forall y \in B(0,r)^c, \phi(y) = 0.$$

Then,

$$\phi \# \mu = \sum_{k=1}^N \mu(B_k \cap B(0,r)) \delta_{y_k} + \mu(B(0,r)^c) \delta_0$$

and

$$\begin{aligned} W_p^p(\phi \# \mu, \mu) &\leq \int_{\mathbb{R}^d} \|y - \phi(y)\|^p d\mu(y) \\ &\leq \epsilon^p \int_{B(0,r)} d\mu(y) + \int_{B(0,r)^c} \|y\|^p d\mu(y) \leq \epsilon^p + \epsilon^p = 2\epsilon^p, \end{aligned}$$

which finishes the proof. ■

Since Dirac masses can be seen as degenerate Gaussian distributions, a direct consequence of Lemma 3.1 is the following proposition.

Proposition 1. $GMM_d(\infty)$ is dense in $\mathcal{P}_p(\mathbb{R}^d)$ for the metric W_p .

3.2. Identifiability properties of Gaussian mixture models. It is clear that Gaussian mixture models are not *stricto sensu* identifiable, since reordering the indexes of a mixture changes its parametrization without changing the underlying probability distribution, or also because a component with mass 1 can be divided in two identical components with masses $\frac{1}{2}$, for example. However, we can show that if we write mixtures in a “compact” way (forbidding two components of the same mixture to be identical), identifiability holds, up to a reordering of the indexes. This property will be useful in the rest of the paper.

Proposition 2. *The set of finite Gaussian mixtures is identifiable, in the sense that two mixtures $\mu_0 = \sum_{k=1}^{K_0} \pi_0^k \mu_0^k$ and $\mu_1 = \sum_{k=1}^{K_1} \pi_1^k \mu_1^k$, written such that all $\{\mu_0^k\}_k$ (resp. all $\{\mu_1^j\}_j$) are pairwise distinct, are equal if and only if $K_0 = K_1$ and we can reorder the indexes such that for all k , $\pi_0^k = \pi_1^k$, $m_0^k = m_1^k$ and $\Sigma_0^k = \Sigma_1^k$.*

Proof. This proof is an adaptation and simplification of the proof of Proposition 2 in [25]. First, assume that $d = 1$ and that two Gaussian mixtures are equal:

$$(3.2) \quad \sum_{k=1}^{K_0} \pi_0^k \mu_0^k = \sum_{j=1}^{K_1} \pi_1^j \mu_1^j.$$

We start by identifying the Dirac masses from both sums, so only non-degenerate Gaussian components remain. Writing $\mu_i^k = \mathcal{N}(m_i^k, (\sigma_i^k)^2)$, it follows that

$$\sum_{k=1}^{K_0} \frac{\pi_0^k}{\sigma_0^k} e^{-\frac{(x-m_0^k)^2}{2(\sigma_0^k)^2}} = \sum_{j=1}^{K_1} \frac{\pi_1^j}{\sigma_1^j} e^{-\frac{(x-m_1^j)^2}{2(\sigma_1^j)^2}}, \quad \forall x \in \mathbb{R}.$$

Now, define $k_0 = \operatorname{argmax}_k \sigma_0^k$ and $j_0 = \operatorname{argmax}_j \sigma_1^j$. If the maximum is attained for several values of k (resp. j), we keep the one with the largest mean $m_0^{k_0}$ (resp. $m_1^{j_0}$). Then, when $x \rightarrow +\infty$, we have the equivalences

$$\sum_{k=1}^{K_0} \frac{\pi_0^k}{\sigma_0^k} e^{-\frac{(x-m_0^k)^2}{2(\sigma_0^k)^2}} \underset{x \rightarrow +\infty}{\sim} \frac{\pi_0^{k_0}}{\sigma_0^{k_0}} e^{-\frac{(x-m_0^{k_0})^2}{2(\sigma_0^{k_0})^2}} \quad \text{and} \quad \sum_{j=1}^{K_1} \frac{\pi_1^j}{\sigma_1^j} e^{-\frac{(x-m_1^j)^2}{2(\sigma_1^j)^2}} \underset{x \rightarrow +\infty}{\sim} \frac{\pi_1^{j_0}}{\sigma_1^{j_0}} e^{-\frac{(x-m_1^{j_0})^2}{2(\sigma_1^{j_0})^2}}.$$

Since the two sums are equal, these two terms must also be equivalent when $x \rightarrow +\infty$, which implies necessarily that $\sigma_0^{k_0} = \sigma_1^{j_0}$, $m_0^{k_0} = m_1^{j_0}$ and $\pi_0^{k_0} = \pi_1^{j_0}$. Now, we can remove these two components from the two sums and we obtain

$$\sum_{k=1 \dots K_0, k \neq k_0} \frac{\pi_0^k}{\sigma_0^k} e^{-\frac{(x-m_0^k)^2}{2(\sigma_0^k)^2}} = \sum_{j=1 \dots K_1, j \neq j_0} \frac{\pi_1^j}{\sigma_1^j} e^{-\frac{(x-m_1^j)^2}{2(\sigma_1^j)^2}}, \quad \forall x \in \mathbb{R}.$$

We can start over and show recursively that all components are equal.

For $d > 1$, assume once again that two Gaussian mixtures μ_0 and μ_1 are equal, written as in Equation (3.2). The projection of this equality yields

$$(3.3) \quad \sum_{k=1}^{K_0} \pi_0^k \mathcal{N}(\langle m_0^k, \xi \rangle, \xi^t \Sigma_0^k \xi) = \sum_{j=1}^{K_1} \pi_1^j \mathcal{N}(\langle m_1^j, \xi \rangle, \xi^t \Sigma_1^j \xi), \quad \forall \xi \in \mathbb{R}^d.$$

At this point, observe that for some values of ξ , some of these projected components may not be pairwise distinct anymore, so we cannot directly apply the result for $d = 1$ to such mixtures. However, since the pairs (m_0^k, Σ_0^k) (resp. (m_1^j, Σ_1^j)) are all distinct, then for $i = 0, 1$, the set

$$\Theta_i = \bigcup_{1 \leq k, k' \leq K_i} \left\{ \xi \text{ s.t. } \langle m_i^k - m_i^{k'}, \xi \rangle = 0 \text{ and } \xi^t (\Sigma_i^k - \Sigma_i^{k'}) \xi = 0 \right\}$$

is of Lebesgue measure 0 in \mathbb{R}^d . For any ξ in $\mathbb{R}^d \setminus \Theta_0 \cup \Theta_1$, the pairs $\{(\langle m_0^k, \xi \rangle, \xi^t \Sigma_0^k \xi)\}_k$ (resp. $\{(\langle m_1^j, \xi \rangle, \xi^t \Sigma_1^j \xi)\}_j$) are pairwise distinct. Consequently, using the first part of the proof (for $d = 1$), we can deduce that $K_0 = K_1$ and that

$$(3.4) \quad \mathbb{R}^d \setminus \Theta_0 \cup \Theta_1 \subset \bigcap_k \bigcup_j \Xi_{k,j}$$

where

$$\Xi_{k,j} = \left\{ \xi, \text{ s.t. } \pi_0^k = \pi_1^j, \langle m_0^k - m_1^j, \xi \rangle = 0 \text{ and } \xi^t (\Sigma_0^k - \Sigma_1^j) \xi = 0 \right\}.$$

Now, assume that the two sets $\{(\pi_0^k, m_0^k, \Sigma_0^k)\}_k$ and $\{(\pi_1^j, m_1^j, \Sigma_1^j)\}_j$ are different. Since each of these sets is composed of different triplets, it is equivalent to assume that there exists k in $\{1, \dots, K_0\}$ such that $(\pi_0^k, m_0^k, \Sigma_0^k)$ is different from all triplets $(\pi_1^j, m_1^j, \Sigma_1^j)$. In this case, the sets $\Xi_{k,j}$ for $j = 1, \dots, K_0$ are all of Lebesgue measure 0 in \mathbb{R}^d , which contradicts (3.4). We conclude that the sets $\{(\pi_0^k, m_0^k, \Sigma_0^k)\}_k$ and $\{(\pi_1^j, m_1^j, \Sigma_1^j)\}_j$ are equal. \blacksquare

3.3. Optimal transport and Wasserstein barycenters between Gaussian Mixture Models. We are now in a position to investigate optimal transport between Gaussian mixture models (GMM). A first important remark is that given two Gaussian mixtures μ_0 and μ_1 on \mathbb{R}^d , optimal transport plans γ between μ_0 and μ_1 are usually not GMM.

Proposition 3. *Let $\mu_0 \in \text{GMM}_d(K_0)$ and $\mu_1 \in \text{GMM}_d(K_1)$ be two Gaussian mixtures such that μ_1 cannot be written $T\#\mu_0$ with T affine. Assume also that μ_0 is absolutely continuous with respect to the Lebesgue measure. Let $\gamma \in \Pi(\mu_0, \mu_1)$ be an optimal transport plan between μ_0 and μ_1 . Then γ does not belong to $\text{GMM}_{2d}(\infty)$.*

Proof. Since μ_0 is absolutely continuous with respect to the Lebesgue measure, we know that the optimal transport plan is unique and is of the form $\gamma = (\text{Id}, T)\#\mu_0$ for a measurable map $T : \mathbb{R}^d \rightarrow \mathbb{R}^d$ that satisfies $T\#\mu_0 = \mu_1$. Thus, if γ belongs to $\text{GMM}_{2d}(\infty)$, all of its components must be degenerate Gaussian distributions $\mathcal{N}(m_k, \Sigma_k)$ such that

$$\cup_k (m_k + \text{Span}(\Sigma_k)) = \text{graph}(T).$$

It follows that T must be affine on \mathbb{R}^d , which contradicts the hypotheses of the proposition. \blacksquare

When μ_0 is not absolutely continuous with respect to the Lebesgue measure (which means that one of its components is degenerate), we cannot write γ under the form (2.2), but we conjecture that the previous result usually still holds. A notable exception is the case where all Gaussian components of μ_0 and μ_1 are Dirac masses on \mathbb{R}^d , in which case γ is also a GMM composed of Dirac masses on \mathbb{R}^{2d} .

We conjecture that since optimal plans γ between two GMM are usually not GMM, the barycenters $(P_t)\#\gamma$ between μ_0 and μ_1 are also usually not GMM either (with the exception of $t = 0, 1$). Take the one dimensional example of $\mu_0 = \mathcal{N}(0, 1)$ and $\mu_1 = \frac{1}{2}(\delta_{-1} + \delta_1)$. Clearly, an optimal transport map between μ_0 and μ_1 is defined as $T(x) = \text{sign}(x)$. For $t \in (0, 1)$, if we denote by μ_t the barycenter between μ_0 with weight $1 - t$ and μ_1 with weight t , then it is easy to show that μ_t has a density

$$f_t(x) = \frac{1}{1-t} \left(g \left(\frac{x+t}{1-t} \right) \mathbf{1}_{x < -t} + g \left(\frac{x-t}{1-t} \right) \mathbf{1}_{x > t} \right),$$

where g is the density of $\mathcal{N}(0, 1)$. The density f_t is equal to 0 on the interval $(-t, t)$ and therefore cannot be the density of a GMM.

4. GW_2 : a distance between Gaussian Mixture Models. In this section, we define a Wasserstein-type distance between Gaussian mixtures ensuring that barycenters between Gaussian mixtures remain Gaussian mixtures. To this aim, we restrict the set of admissible transport plans to Gaussian mixtures and show that the problem is well defined. Thanks to the identifiability results proved in the previous section, we will show that the corresponding optimization problem boils down to a very simple discrete formulation.

4.1. Definition of GW_2 .

Definition 2. Let μ_0 and μ_1 be two Gaussian mixtures. We define

$$(4.1) \quad GW_2^2(\mu_0, \mu_1) := \inf_{\gamma \in \Pi(\mu_0, \mu_1) \cap GMM_{2d}(\infty)} \int_{\mathbb{R}^d \times \mathbb{R}^d} \|y_0 - y_1\|^2 d\gamma(y_0, y_1).$$

First, observe that the problem is well defined since $\Pi(\mu_0, \mu_1) \cap GMM_{2d}(\infty)$ contains at least the product measure $\mu_0 \otimes \mu_1$. Notice also that from the definition we directly have that

$$GW_2(\mu_0, \mu_1) \geq W_2(\mu_0, \mu_1).$$

4.2. An equivalent discrete formulation. Now, we can show that this optimisation problem has a very simple discrete formulation. For $\pi_0 \in \Gamma_{K_0}$ and $\pi_1 \in \Gamma_{K_1}$, we denote by $\Pi(\pi_0, \pi_1)$ the subset of the simplex $\Gamma_{K_0 \times K_1}$ with marginals π_0 and π_1 , *i.e.*

$$(4.2) \quad \Pi(\pi_0, \pi_1) = \{w \in \mathcal{M}_{K_0, K_1}(\mathbb{R}^+); w \mathbf{1}_{K_1} = \pi_0; w^t \mathbf{1}_{K_0} = \pi_1\}$$

$$(4.3) \quad = \{w \in \mathcal{M}_{K_0, K_1}(\mathbb{R}^+); \forall k, \sum_j w_{kj} = \pi_0^k \text{ and } \forall j, \sum_k w_{kj} = \pi_1^j\}.$$

Proposition 4. Let $\mu_0 = \sum_{k=1}^{K_0} \pi_0^k \mu_0^k$ and $\mu_1 = \sum_{k=1}^{K_1} \pi_1^k \mu_1^k$ be two Gaussian mixtures, then

$$(4.4) \quad GW_2^2(\mu_0, \mu_1) = \min_{w \in \Pi(\pi_0, \pi_1)} \sum_{k,l} w_{kl} W_2^2(\mu_0^k, \mu_1^l).$$

Moreover, if w^* is a minimizer of (4.4), and if $T_{k,l}$ is the W_2 -optimal map between μ_0^k and μ_1^l , then γ^* defined as

$$\gamma^*(x, y) = \sum_{k,l} w_{kl}^* g_{m_0^k, \Sigma_0^k}(x) \delta_{y=T_{k,l}(x)}$$

is a minimizer of (4.1).

Proof. First, let w^* be a solution of the linear program

$$(4.5) \quad \inf_{w \in \Pi(\pi_0, \pi_1)} \sum_{k,l} w_{kl} W_2^2(\mu_0^k, \mu_1^l).$$

For each pair (k, l) , let

$$\gamma_{kl} = \operatorname{argmin}_{\gamma \in \Pi(\mu_0^k, \mu_1^l)} \int_{\mathbb{R}^d \times \mathbb{R}^d} \|y_0 - y_1\|^2 d\gamma(y_0, y_1)$$

and

$$\gamma^* = \sum_{k,l} w_{kl}^* \gamma_{kl}.$$

Clearly, $\gamma^* \in \Pi(\mu_0, \mu_1) \cap GMM_{2d}(K_0 K_1)$. It follows that

$$\begin{aligned} \sum_{k,l} w_{kl}^* W_2^2(\mu_0^k, \mu_1^l) &= \int_{\mathbb{R}^d \times \mathbb{R}^d} \|y_0 - y_1\|^2 d\gamma^*(y_0, y_1) \\ &\geq \min_{\gamma \in \Pi(\mu_0, \mu_1) \cap GMM_{2d}(K_0 K_1)} \int_{\mathbb{R}^d \times \mathbb{R}^d} \|y_0 - y_1\|^2 d\gamma(y_0, y_1) \\ &\geq \min_{\gamma \in \Pi(\mu_0, \mu_1) \cap GMM_{2d}(\infty)} \int_{\mathbb{R}^d \times \mathbb{R}^d} \|y_0 - y_1\|^2 d\gamma(y_0, y_1), \end{aligned}$$

because $GMM_{2d}(K_0 K_1) \subset GMM_{2d}(\infty)$.

Now, let γ be any element of $\Pi(\mu_0, \mu_1) \cap GMM_{2d}(\infty)$. Since γ belongs to $GMM_{2d}(\infty)$, there exists an integer K such that $\gamma = \sum_{j=1}^K w_j \gamma_j$. Since $P_0 \# \gamma = \mu_0$, it follows that

$$\sum_{j=1}^K w_j P_0 \# \gamma_j = \sum_{k=1}^{K_0} \pi_0^k \mu_0^k.$$

Thanks to the identifiability property shown in the previous section, we know that these two Gaussian mixtures must have the same components, so for each j in $\{1, \dots, K\}$, there is $1 \leq k \leq K_0$ such that $P_0 \# \gamma_j = \mu_0^k$. In the same way, there is $1 \leq l \leq K_1$ such that $P_1 \# \gamma_j = \mu_1^l$. It follows that γ_j belongs to $\Pi(\mu_0^k, \mu_1^l)$. We conclude that the mixture γ can be written as a mixture of Gaussian components $\gamma_{kl} \in \Pi(\mu_0^k, \mu_1^l)$, i.e. $\gamma = \sum_{k=1}^{K_0} \sum_{l=1}^{K_1} w_{kl} \gamma_{kl}$. Since $P_0 \# \gamma = \mu_0$ and $P_1 \# \gamma = \mu_1$, we know that $w \in \Pi(\pi_0, \pi_1)$. As a consequence,

$$\int_{\mathbb{R}^d \times \mathbb{R}^d} \|y_0 - y_1\|^2 d\gamma(y_0, y_1) \geq \sum_{k=1}^{K_0} \sum_{l=1}^{K_1} w_{kl} W_2^2(\mu_0^k, \mu_1^l) \geq \sum_{k=1}^{K_0} \sum_{l=1}^{K_1} w_{kl}^* W_2^2(\mu_0^k, \mu_1^l).$$

This inequality holds for any γ in $\Pi(\mu_0, \mu_1) \cap GMM_{2d}(\infty)$, which concludes the proof. \blacksquare

The discrete form (4.4) has been recently proposed as an ingenious alternative to W_2 in the machine learning literature [5, 6]. Under this form, however, it was not obvious that the definition was not ambiguous, in the sense that the value of the minimum is the same

whatever the parametrization of the Gaussian mixtures μ_0 and μ_1 . Definition (4.1) clarifies this question.

Observe also that we do not use in the definition and in the proof the fact that the ground cost is quadratic. Definition 2 can easily be generalized to other cost functions $c : \mathbb{R}^{2d} \mapsto \mathbb{R}$. The reason why we focus on the quadratic cost is that optimal transport plans between Gaussian measures for W_2 can be computed explicitly. It follows from the equivalence between the continuous and discrete forms of GW_2 that the solution of (4.1) is very easy to compute in practice. Another consequence of this equivalence is that there exists at least one optimal plan γ^* for (4.1) containing less than $K_0 + K_1 - 1$ Gaussian components.

Corollary 1. *Let $\mu_0 = \sum_{k=1}^{K_0} \pi_0^k \mu_0^k$ and $\mu_1 = \sum_{k=1}^{K_1} \pi_1^k \mu_1^k$ be two Gaussian mixtures on \mathbb{R}^d , then the infimum in (4.1) is attained for a given $\gamma^* \in \Pi(\mu_0, \mu_1) \cap GMM_{2d}(K_0 + K_1 - 1)$.*

Proof. This follows directly from the proof that there exists at least one optimal w^* for (4.1) containing less than $K_0 + K_1 - 1$ Gaussian components (see [15]). ■

4.3. An example in one dimension. In order to illustrate the behavior of the optimal maps for GW_2 , we focus here on a very simple example in one dimension, where μ_0 and μ_1 are the following mixtures of two Gaussian components

$$\mu_0 = 0.3\mathcal{N}(0.2, 0.03) + 0.7\mathcal{N}(0.4, 0.04),$$

$$\mu_1 = 0.6\mathcal{N}(0.6, 0.06) + 0.4\mathcal{N}(0.8, 0.07).$$

Figure 1 shows the optimal transport plans between μ_0 (in blue) and μ_1 (in red), both for the Wasserstein distance W_2 and for GW_2 . As we can observe, the optimal transport plan for GW_2 (a probability measure on $\mathbb{R} \times \mathbb{R}$) is a mixture of three degenerate Gaussian measures supported by 1D lines.

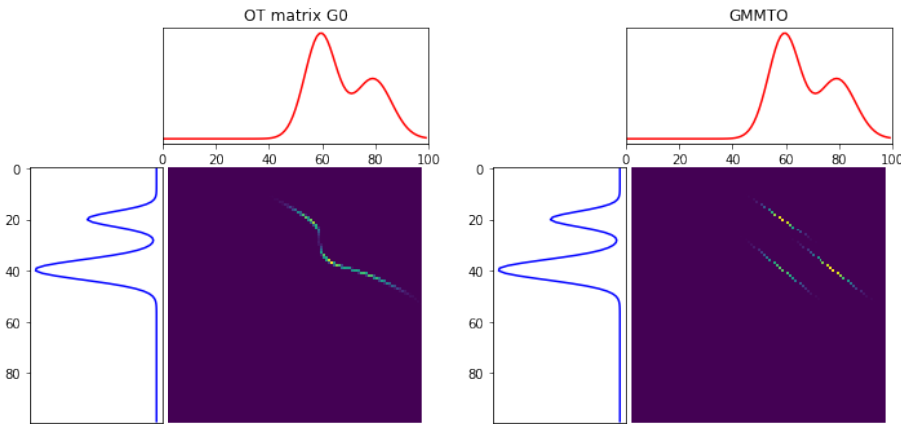


Figure 1. *Transport plans between two mixtures of Gaussians μ_0 (in blue) and μ_1 (in red). Left, optimal transport plan for W_2 . Right, optimal transport plan for GW_2 . These examples have been computed using the Python Optimal Transport (POT) library [10].*

4.4. Metric properties of GW_2 and displacement interpolation.

4.4.1. Metric properties of GW_2 .

Proposition 5. GW_2 defines a metric on $GMM_d(\infty)$ and the space $GMM_d(\infty)$ equipped with the distance GW_2 is a geodesic space.

This proposition can be proved very easily by making use of the discrete formulation (4.4) of the distance (see for instance [5]). For the sake of completeness, we provide in the following a proof of the proposition using only the continuous formulation of GW_2 .

Proof. First, observe that GW_2 is obviously symmetric and positive. It is also clear that for any Gaussian mixture μ , $GW_2(\mu, \mu) = 0$. Conversely, assume that $GW_2(\mu_0, \mu_1) = 0$, it implies that $W_2(\mu_0, \mu_1) = 0$ and thus $\mu_0 = \mu_1$ since W_2 is a distance.

It remains to show that GW_2 satisfies the triangle inequality. This is a classical consequence of the gluing lemma, but we must be careful to check that the constructed measure remains a Gaussian mixture. Let μ_0, μ_1, μ_2 be three Gaussian mixtures on \mathbb{R}^d . Let γ_{01} and γ_{12} be optimal plans respectively for (μ_0, μ_1) and (μ_1, μ_2) for the problem GW_2 (which means that γ_{01} and γ_{12} are both GMM on \mathbb{R}^{2d}). The classical gluing lemma consists in disintegrating γ_{01} and γ_{12} into

$$d\gamma_{01}(y_0, y_1) = d\gamma_{01}(y_0|y_1)d\mu_1(y_1) \quad \text{and} \quad d\gamma_{12}(y_1, y_2) = d\gamma_{12}(y_2|y_1)d\mu_1(y_1),$$

and to define

$$d\gamma_{012}(y_0, y_1, y_2) = d\gamma_{01}(y_0|y_1)d\mu_1(y_1)d\gamma_{12}(y_2|y_1),$$

which boils down to assume independence conditionally to the value of y_1 . Since γ_{01} and γ_{12} are Gaussian mixtures on \mathbb{R}^{2d} , the conditional distributions $d\gamma_{01}(y_0|y_1)$ and $d\gamma_{12}(y_2|y_1)$ are also Gaussian mixtures for all y_1 in the support of μ_1 (recalling that μ_1 is the marginal on y_1 of both γ_{01} and γ_{12}). If we define a distribution γ_{02} by integrating γ_{012} over the variable y_1 , *i.e.*

$$d\gamma_{02}(y_0, y_2) = \int_{y_1 \in \mathbb{R}^d} d\gamma_{012}(y_0, y_1, y_2) = \int_{y_1 \in \text{Supp}(\mu_1)} d\gamma_{01}(y_0|y_1)d\mu_1(y_1)d\gamma_{12}(y_2|y_1)$$

then γ_{02} is obviously also a Gaussian mixture on \mathbb{R}^{2d} with marginals μ_0 and μ_2 . The rest of the proof is classical. Indeed, we can write

$$GW_2^2(\mu_0, \mu_2) \leq \int_{\mathbb{R}^d \times \mathbb{R}^d} \|y_0 - y_2\|^2 d\gamma_{02}(y_0, y_2) = \int_{\mathbb{R}^d \times \mathbb{R}^d \times \mathbb{R}^d} \|y_0 - y_2\|^2 d\gamma_{012}(y_0, y_1, y_2).$$

Writing $\|y_0 - y_2\|^2 = \|y_0 - y_1\|^2 + \|y_1 - y_2\|^2 + 2\langle y_0 - y_1, y_1 - y_2 \rangle$ (with $\langle \cdot, \cdot \rangle$ the Euclidean scalar product on \mathbb{R}^d), and using the Cauchy-Schwarz inequality, it follows that

$$GW_2^2(\mu_0, \mu_2) \leq \left(\sqrt{\int_{\mathbb{R}^{2d}} \|y_0 - y_1\|^2 d\gamma_{01}(y_0, y_1)} + \sqrt{\int_{\mathbb{R}^{2d}} \|y_1 - y_2\|^2 d\gamma_{12}(y_1, y_2)} \right)^2.$$

The triangle inequality follows by taking for γ_{01} (resp. γ_{12}) the optimal plan for GW_2 between μ_0 and μ_1 (resp. μ_1 and μ_2).

Now, let us show that $GMM_d(\infty)$ equipped with the distance GW_2 is a geodesic space. For a path $\rho = (\rho_t)_{t \in [0,1]}$ in $GMM_d(\infty)$ (meaning that each ρ_t is a GMM on \mathbb{R}^d), we can define its length for GW_2 by

$$\text{Len}_{GW_2}(\rho) = \text{Sup}_{N; 0=t_0 \leq t_1 \dots \leq t_N=1} \sum_{i=1}^N GW_2(\rho_{t_{i-1}}, \rho_{t_i}) \in [0, +\infty].$$

Let $\mu_0 = \sum_k \pi_0^k \mu_0^k$ and $\mu_1 = \sum_l \pi_1^l \mu_1^l$ be two GMM. Since GW_2 satisfies the triangle inequality, we always have that $\text{Len}_{GW_2}(\rho) \geq GW_2(\mu_0, \mu_1)$ for all paths ρ such that $\rho_0 = \mu_0$ and $\rho_1 = \mu_1$. To prove that $(GMM_d(\infty), GW_2)$ is a geodesic space we just have to exhibit a path ρ connecting μ_0 to μ_1 and such that its length is equal to $GW_2(\mu_0, \mu_1)$.

We write γ^* the optimal transport plan between μ_0 and μ_1 . For $t \in (0, 1)$ we can define

$$\mu_t = (P_t) \# \gamma^*.$$

Let $t < s \in [0, 1]$ and define $\gamma_{t,s}^* = (P_t, P_s) \# \gamma^*$. Then $\gamma_{t,s}^* \in \Pi(\mu_t, \mu_s) \cap GMM_{2d}(\infty)$ and therefore

$$\begin{aligned} GW_2(\mu_t, \mu_s)^2 &= \min_{\tilde{\gamma} \in \Pi(\mu_t, \mu_s) \cap GMM_{2d}(\infty)} \iint \|y_0 - y_1\|^2 d\tilde{\gamma}(y_0, y_1) \\ &\leq \iint \|y_0 - y_1\|^2 d\gamma_{t,s}^*(y_0, y_1) = \iint \|P_t(y_0, y_1) - P_s(y_0, y_1)\|^2 d\gamma^*(y_0, y_1) \\ &= \iint \|(1-t)y_0 + ty_1 - (1-s)y_0 - sy_1\|^2 d\gamma^*(y_0, y_1) \\ &= (s-t)^2 GW_2(\mu_0, \mu_1)^2. \end{aligned}$$

Thus we have that $GW_2(\mu_t, \mu_s) \leq (s-t)GW_2(\mu_0, \mu_1)$. Now, by the triangle inequality,

$$\begin{aligned} GW_2(\mu_0, \mu_1) &\leq GW_2(\mu_0, \mu_t) + GW_2(\mu_t, \mu_s) + GW_2(\mu_s, \mu_1) \\ &\leq (t + s - t + 1 - s)GW_2(\mu_0, \mu_1). \end{aligned}$$

Therefore all inequalities are equalities, and $GW_2(\mu_t, \mu_s) = (s-t)GW_2(\mu_0, \mu_1)$ for all $0 \leq t \leq s \leq 1$. This implies that the GW_2 length of the path $(\mu_t)_t$ is equal to $GW_2(\mu_0, \mu_1)$. It allows us to conclude that $(GMM_d(\infty), GW_2)$ is a geodesic space, and we have also given the explicit expression of the geodesic. \blacksquare

The following Corollary is a direct consequence of the previous results.

Corollary 2. *The barycenters between $\mu_0 = \sum_k \pi_0^k \mu_0^k$ and $\mu_1 = \sum_l \pi_1^l \mu_1^l$ all belong to $GMM_d(\infty)$ and can be written explicitly as*

$$\forall t \in [0, 1], \quad \mu_t = P_t \# \gamma^* = \sum_{k,l} w_{k,l}^* \mu_t^{k,l},$$

where w^* is an optimal solution of (4.4), and $\mu_t^{k,l}$ is the displacement interpolation between μ_0^k and μ_1^l . When Σ_0^k is non-singular, it is given by

$$\mu_t^{k,l} = ((1-t)\text{Id} + tT_{k,l}) \# \mu_0^k,$$

with $T_{k,l}$ the affine transport map between μ_0^k and μ_1^l given by Equation (2.9). These barycenters have less than $K_0 + K_1 - 1$ components.

4.4.2. 1D and 2D barycenter examples.

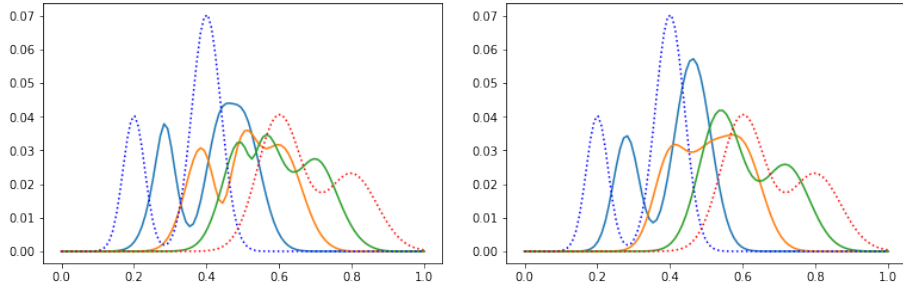


Figure 2. Barycenters μ_t between two Gaussian mixtures μ_0 (blue dotted curve) and μ_1 (red dotted curve). On the left, barycenters for the metric W_2 . On the right, barycenters for the metric GW_2 . The barycenters are computed for $t = 0.25, 0.5$ and 0.75 .

One dimensional case. Figure 2 shows barycenters μ_t for $t = 0.25, 0.5$ and 0.75 between the μ_0 and μ_1 defined in Section 4.3, for both the metric W_2 and GW_2 . Observe that the barycenters computed for GW_2 are a bit more regular (we know that they are mixtures of at most 3 Gaussian components) than those obtained for W_2 .

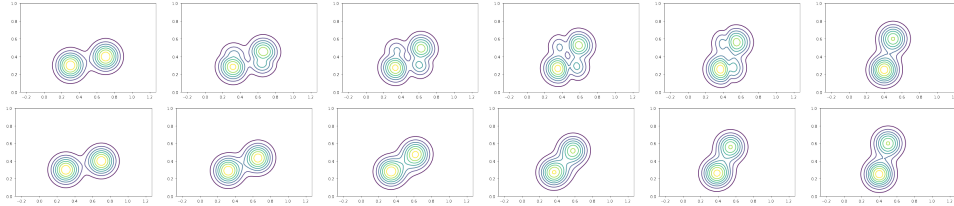


Figure 3. Barycenters μ_t between two Gaussian mixtures μ_0 (first column) and μ_1 (last column). Top: barycenters for the metric W_2 . Bottom: barycenters for the metric GW_2 . The barycenters are computed for $t = 0.0, 0.2, 0.4, 0.6, 0.8, 1.0$.

Two dimensional case. Figure 3 shows barycenters μ_t between the following two dimensional mixtures

$$\mu_0 = 0.5\mathcal{N}\left(\begin{pmatrix} 0.3 \\ 0.3 \end{pmatrix}, 0.01I_2\right) + 0.5\mathcal{N}\left(\begin{pmatrix} 0.7 \\ 0.4 \end{pmatrix}, 0.01I_2\right),$$

$$\mu_1 = 0.45\mathcal{N}\left(\begin{pmatrix} 0.5 \\ 0.6 \end{pmatrix}, 0.01I_2\right) + 0.55\mathcal{N}\left(\begin{pmatrix} 0.4 \\ 0.25 \end{pmatrix}, 0.01I_2\right),$$

where I_2 is the 2×2 identity matrix. Notice that the GW_2 geodesic looks like a simple displacement of both Gaussians to new positions, even if some mass is transferred from one to the other since $\pi_0 \neq \pi_1$. In the W_2 geodesic, we clearly see that the mass of each Gaussian is splitted in two halves which are displaced to the two final Gaussian components.

5. Comparison between GW_2 and W_2 .

Proposition 6. *Let $\mu_0 \in GMM_d(K_0)$ and $\mu_1 \in GMM_d(K_1)$ be two Gaussian mixtures, written as in (3.1). Then,*

$$W_2(\mu_0, \mu_1) \leq GW_2(\mu_0, \mu_1) \leq W_2(\mu_0, \mu_1) + \sum_{i=0,1} \left(2 \sum_{k=1}^{K_i} \pi_i^k \text{trace}(\Sigma_i^k) \right)^{\frac{1}{2}}.$$

The left-hand side inequality is attained when for instance

- μ_0 and μ_1 are both composed of only one Gaussian component,
- μ_0 and μ_1 are finite linear combinations of Dirac masses,
- μ_1 is obtained from μ_0 by an affine transformation.

As we already noticed it, the first inequality is obvious and follows from the definition of GW_2 . It might not be completely intuitive that GW_2 can indeed be strictly larger than W_2 because of the density property of $GMM_d(\infty)$ in $\mathcal{P}_2(\mathbb{R}^d)$. This follows from the fact that our optimization problem has constraints $\gamma \in \Pi(\mu_0, \mu_1)$. Even if any measure γ in $\Pi(\mu_0, \mu_1)$ can be approximated by a sequence of Gaussian mixtures, this sequence of Gaussian mixtures will generally not belong to $\Pi(\mu_0, \mu_1)$, hence explaining the difference between GW_2 and W_2 .

In order to show that GW_2 is always smaller than the sum of W_2 plus a term depending on the trace of the covariance matrices of the two Gaussian mixtures, we start with a lemma which makes more explicit the distance GW_2 between a Gaussian mixture and a mixture of Dirac distributions.

Lemma 5.1. *Let $\mu_0 = \sum_{k=1}^{K_0} \pi_0^k \mu_0^k$ with $\mu_0^k = \mathcal{N}(m_0^k, \Sigma_0^k)$ and $\mu_1 = \sum_{k=1}^{K_1} \pi_1^k \delta_{m_1^k}$. Let $\tilde{\mu}_0 = \sum_{k=1}^{K_0} \pi_0^k \delta_{m_0^k}$ ($\tilde{\mu}_0$ only retains the means of μ_0). Then,*

$$GW_2^2(\mu_0, \mu_1) = W_2^2(\tilde{\mu}_0, \mu_1) + \sum_{k=1}^{K_0} \pi_0^k \text{trace}(\Sigma_0^k).$$

Proof.

$$\begin{aligned} GW_2^2(\mu_0, \mu_1) &= \inf_{w \in \Pi(\pi_0, \pi_1)} \sum_{k,l} w_{kl} W_2^2(\mu_0^k, \delta_{m_1^l}) = \inf_{w \in \Pi(\pi_0, \pi_1)} \sum_{k,l} w_{kl} \left(\|m_1^l - m_0^k\|^2 + \text{trace}(\Sigma_0^k) \right) \\ &= \inf_{w \in \Pi(\pi_0, \pi_1)} \sum_{k,l} w_{kl} \|m_1^l - m_0^k\|^2 + \sum_k \pi_0^k \text{trace}(\Sigma_0^k) = W_2^2(\tilde{\mu}_0, \mu_1) + \sum_{k=1}^{K_0} \pi_0^k \text{trace}(\Sigma_0^k). \end{aligned}$$

In other words, the squared distance GW_2^2 between μ_0 and μ_1 is the sum of the squared Wasserstein distance between $\tilde{\mu}_0$ and μ_1 and a linear combination of the traces of the covariance matrices of the components of μ_0 . We are now in a position to show the other inequality between GW_2 and W_2 .

Proof of Proposition 6. Let $(\mu_0^n)_n$ and $(\mu_1^n)_n$ be two sequences of mixtures of Dirac masses respectively converging to μ_0 and μ_1 in $\mathcal{P}_2(\mathbb{R}^d)$. Since GW_2 is a distance,

$$\begin{aligned} GW_2(\mu_0, \mu_1) &\leq GW_2(\mu_0^n, \mu_1^n) + GW_2(\mu_0, \mu_0^n) + GW_2(\mu_1, \mu_1^n) \\ &= W_2(\mu_0^n, \mu_1^n) + GW_2(\mu_0, \mu_0^n) + GW_2(\mu_1, \mu_1^n). \end{aligned}$$

We study in the following the limits of these three terms when $n \rightarrow +\infty$.

First, observe that $GW_2(\mu_0^n, \mu_1^n) = W_2(\mu_0^n, \mu_1^n) \xrightarrow{n \rightarrow \infty} W_2(\mu_0, \mu_1)$ since W_2 is continuous on $\mathcal{P}_2(\mathbb{R}^d)$.

Second, using Lemma 5.1, for $i = 0, 1$,

$$GW_2^2(\mu_i, \mu_i^n) = W_2^2(\tilde{\mu}_i, \mu_i^n) + \sum_{k=1}^{K_i} \pi_i^k \text{trace}(\Sigma_i^k) \xrightarrow{n \rightarrow \infty} W_2^2(\tilde{\mu}_i, \mu_i) + \sum_{k=1}^{K_i} \pi_i^k \text{trace}(\Sigma_i^k).$$

Define the measure $d\gamma(x, y) = \sum_{k=1}^{K_i} \pi_i^k \delta_{m_i^k}(y) g_{m_i^k, \Sigma_i^k}(x) dx$, with $g_{m_i^k, \Sigma_i^k}$ the probability density function of the Gaussian distribution $\mathcal{N}(m_i^k, \Sigma_i^k)$. The probability measure γ belongs to $\Pi(\mu_i, \tilde{\mu}_i)$, so

$$\begin{aligned} W_2^2(\mu_i, \tilde{\mu}_i) &\leq \int \|x - y\|^2 d\gamma(x, y) = \sum_{k=1}^{K_i} \pi_i^k \int_{\mathbb{R}^d} \|x - m_i^k\|^2 g_{m_i^k, \Sigma_i^k}(x) dx \\ &= \sum_{k=1}^{K_i} \pi_i^k \text{trace}(\Sigma_i^k). \end{aligned}$$

We conclude that

$$\begin{aligned} GW_2(\mu_0, \mu_1) &\leq \liminf_{n \rightarrow \infty} (W_2(\mu_0^n, \mu_1^n) + GW_2(\mu_0, \mu_0^n) + GW_2(\mu_1, \mu_1^n)) \\ &\leq W_2(\mu_0, \mu_1) + \left(W_2^2(\tilde{\mu}_0, \mu_0) + \sum_{k=1}^{K_0} \pi_0^k \text{trace}(\Sigma_0^k) \right)^{\frac{1}{2}} + \left(W_2^2(\tilde{\mu}_1, \mu_1) + \sum_{k=1}^{K_1} \pi_1^k \text{trace}(\Sigma_1^k) \right)^{\frac{1}{2}} \\ &\leq W_2(\mu_0, \mu_1) + \left(2 \sum_{k=1}^{K_0} \pi_0^k \text{trace}(\Sigma_0^k) \right)^{\frac{1}{2}} + \left(2 \sum_{k=1}^{K_1} \pi_1^k \text{trace}(\Sigma_1^k) \right)^{\frac{1}{2}}. \end{aligned}$$

This ends the proof of the proposition.

Observe that if μ is a Gaussian distribution $\mathcal{N}(m, \Sigma)$ and μ^n a distribution supported by a finite number of points which converges to μ in $\mathcal{P}_2(\mathbb{R}^d)$, then

$$W_2^2(\mu, \mu^n) \xrightarrow{n \rightarrow \infty} 0$$

and

$$GW_2(\mu, \mu^n) = (W_2^2(\tilde{\mu}, \mu^n) + \text{trace}(\Sigma))^{\frac{1}{2}} \xrightarrow{n \rightarrow \infty} (2\text{trace}(\Sigma))^{\frac{1}{2}} \neq 0.$$

Let us also remark that if μ_0 and μ_1 are Gaussian mixtures such that $\max_{k,i} \text{trace}(\Sigma_i^k) \leq \varepsilon$, then

$$GW_2(\mu_0, \mu_1) \leq W_2(\mu_0, \mu_1) + 2\sqrt{2\varepsilon}.$$

6. Multi-marginal formulation and barycenters.

6.1. Multi-marginal formulation for GW_2 . Let $\mu_0, \mu_1, \dots, \mu_{J-1}$ be J Gaussian mixtures on \mathbb{R}^d , and let $\lambda_0, \dots, \lambda_{J-1}$ be J positive weights summing to 1. The multi-marginal version of our optimal transport problem restricted to Gaussian mixture models can be written

$$(6.1) \quad MGW_2(\mu_0, \dots, \mu_{J-1}) := \inf_{\gamma \in \Pi(\mu_0, \dots, \mu_{J-1}) \cap GMM_{Jd}(\infty)} \int_{\mathbb{R}^{dJ}} c(x_0, \dots, x_{J-1}) d\gamma(x_0, \dots, x_{J-1}),$$

where

$$(6.2) \quad c(x_0, \dots, x_{J-1}) = \sum_{i=0}^{J-1} \lambda_i \|x_i - B(x)\|^2 = \frac{1}{2} \sum_{i,j=0}^{J-1} \lambda_i \lambda_j \|x_i - x_j\|^2$$

and where $\Pi(\mu_0, \mu_1, \dots, \mu_{J-1})$ is the set of probability measures on $(\mathbb{R}^d)^J$ having $\mu_0, \mu_1, \dots, \mu_{J-1}$ as marginals.

Writing for every j , $\mu_j = \sum_{k=1}^{K_j} \pi_j^k \mu_j^k$, and using exactly the same arguments as in Proposition 4, we can easily show the following result.

Proposition 7. *The optimisation problem (6.1) can be rewritten under the discrete form*

$$(6.3) \quad MGW_2(\mu_0, \dots, \mu_{J-1}) = \min_{w \in \Pi(\pi_0, \dots, \pi_{J-1})} \sum_{k_0, \dots, k_{J-1}=1}^{K_0, \dots, K_{J-1}} w_{k_0 \dots k_{J-1}} MW_2^2(\mu_0^{k_0}, \dots, \mu_{J-1}^{k_{J-1}}),$$

where $\Pi(\pi_0, \pi_1, \dots, \pi_{J-1})$ is the subset of tensors w in $\mathcal{M}_{K_0, K_1, \dots, K_{J-1}}(\mathbb{R}^+)$ having $\pi_0, \pi_1, \dots, \pi_{J-1}$ as discrete marginals, i.e. such that

$$(6.4) \quad \forall j \in \{0, \dots, J-1\}, \forall k \in \{1, \dots, K_j\}, \sum_{\substack{1 \leq k_0 \leq K_0 \\ \dots \\ 1 \leq k_{j-1} \leq K_{j-1} \\ k_j = k \\ 1 \leq k_{j+1} \leq K_{j+1} \\ \dots \\ 1 \leq k_{J-1} \leq K_{J-1}}} w_{k_0 k_1 \dots k_{J-1}} = \pi_j^k.$$

Moreover, the solution γ^* of (6.1) can be written

$$(6.5) \quad \gamma^* = \sum_{\substack{1 \leq k_0 \leq K_0 \\ \dots \\ 1 \leq k_{J-1} \leq K_{J-1}}} w_{k_0 k_1 \dots k_{J-1}}^* \gamma_{k_0 k_1 \dots k_{J-1}}^*,$$

where w^* is solution of (6.3) and $\gamma_{k_0 k_1 \dots k_{J-1}}^*$ is the optimal multi-marginal plan between the Gaussian measures $\mu_0^{k_0}, \dots, \mu_{J-1}^{k_{J-1}}$ (see Section 2.5.2).

From Section 2.5.2, we know how to construct the optimal multi-marginal plans $\gamma_{k_0 k_1 \dots k_{J-1}}^*$, which means that computing a solution for (6.1) boils down to solve the linear program (6.3) in order to find w^* .

6.2. Link with the GW_2 -barycenters. We will now show the link between the previous multi-marginal problem and the barycenters for GW_2 .

Proposition 8. *The barycenter problem*

$$(6.6) \quad \inf_{\nu \in GMM_d(\infty)} \sum_{j=0}^{J-1} \lambda_j GW_2^2(\mu_j, \nu),$$

has a solution given by $\nu^* = B\#\gamma^*$, where γ^* is an optimal plan for the multi-marginal problem (6.1).

Proof. For any $\gamma \in \Pi(\mu_0, \dots, \mu_{J-1}) \cap GMM_{Jd}(\infty)$, we define $\gamma_j = (P_j, B)\#\gamma$, with B the barycenter application defined in (2.4) and $P_j : (\mathbb{R}^d)^J \mapsto \mathbb{R}^d$ such that $P(x_0, \dots, x_{J-1}) = x_j$. Observe that γ_j belongs to $\Pi(\mu_j, \nu)$ with $\nu = B\#\gamma$. The probability measure γ_j also belongs to $GMM_{2d}(\infty)$ since (P_j, B) is a linear application. It follows that

$$\begin{aligned} \int_{(\mathbb{R}^d)^J} \sum_{j=0}^{J-1} \lambda_j \|x_j - B(x)\|^2 d\gamma(x_0, \dots, x_{J-1}) &= \sum_{j=0}^{J-1} \lambda_j \int_{(\mathbb{R}^d)^J} \|x_j - B(x)\|^2 d\gamma(x_0, \dots, x_{J-1}) \\ &= \sum_{j=0}^{J-1} \lambda_j \int_{\mathbb{R}^d \times \mathbb{R}^d} \|x_j - y\|^2 d\gamma_j(x_j, y) \\ &\geq \sum_{j=0}^{J-1} \lambda_j GW_2^2(\mu_j, \nu). \end{aligned}$$

This inequality holds for any arbitrary $\gamma \in \Pi(\mu_0, \dots, \mu_{J-1}) \cap GMM_{Jd}(\infty)$, thus

$$MGW_2(\mu_0, \dots, \mu_{J-1}) \geq \inf_{\nu \in GMM_d(\infty)} \sum_{j=0}^{J-1} \lambda_j GW_2^2(\mu_j, \nu).$$

Conversely, for any ν in $GMM_d(\infty)$, we can write $\nu = \sum_{l=1}^L \pi_\nu^l \nu^l$, the ν^l being Gaussian probability measures. We also write $\mu_j = \sum_{k=1}^{K_j} \pi_j^k \mu_j^k$, and we call w^j the optimal discrete plan for GW_2 between the mixtures μ_j and ν (see Equation (4.4)). Then,

$$\sum_{j=0}^{J-1} \lambda_j GW_2^2(\mu_j, \nu) = \sum_{j=0}^{J-1} \lambda_j \sum_{k,l} w_{k,l}^j W_2^2(\mu_j^k, \nu^l).$$

Now, if we define a $K_0 \times \dots \times K_{J-1} \times L$ tensor α and a $K_0 \times \dots \times K_{J-1}$ tensor $\bar{\alpha}$ by

$$\alpha_{k_0 \dots k_{J-1} l} = \frac{\prod_{j=0}^{J-1} w_{k_j, l}^j}{(\pi_\nu^l)^{J-1}} \quad \text{and} \quad \bar{\alpha}_{k_0 \dots k_{J-1}} = \sum_{l=1}^L \alpha_{k_0 \dots k_{J-1} l},$$

clearly $\alpha \in \Pi(\pi_0, \dots, \pi_{J-1}, \pi_\nu)$ and $\bar{\alpha} \in \Pi(\pi_0, \dots, \pi_{J-1})$. Moreover,

$$\begin{aligned}
\sum_{j=0}^{J-1} \lambda_j GW_2^2(\mu_j, \nu) &= \sum_{j=0}^{J-1} \lambda_j \sum_{k_j=1}^{K_j} \sum_{l=1}^L w_{k_j, l}^j W_2^2(\mu_j^{k_j}, \nu^l) \\
&= \sum_{j=0}^{J-1} \lambda_j \sum_{k_1, \dots, k_{J-1}, l} \alpha_{k_0 \dots k_{J-1} l} W_2^2(\mu_j^{k_j}, \nu^l) \\
&= \sum_{k_1, \dots, k_{J-1}, l} \alpha_{k_0 \dots k_{J-1} l} \sum_{j=0}^{J-1} \lambda_j W_2^2(\mu_j^{k_j}, \nu^l) \\
&\geq \sum_{k_1, \dots, k_{J-1}, l} \alpha_{k_0 \dots k_{J-1} l} MW_2^2(\mu_0^{k_0}, \dots, \mu_{J-1}^{k_{J-1}}) \quad (\text{see Equation (2.7)}) \\
&= \sum_{k_1, \dots, k_{J-1}} \bar{\alpha}_{k_0 \dots k_{J-1}} MW_2^2(\mu_0^{k_0}, \dots, \mu_{J-1}^{k_{J-1}}) \geq MGW_2^2(\mu_0, \dots, \mu_{J-1}),
\end{aligned}$$

the last inequality being a consequence of Proposition 7. Since this holds for any arbitrary ν in $GMM_d(\infty)$, this ends the proof. \blacksquare

The following corollary gives a more explicit formulation for the barycenters for GW_2 , and shows that the number of Gaussian components in the mixture is much smaller than $\prod_{j=0}^{J-1} K_j$.

Corollary 3. *Let μ_0, \dots, μ_{J-1} be J Gaussian mixtures such that all the involved covariance matrices are positive definite, then the solution of (6.8) can be written*

$$(6.7) \quad \nu = \sum_{k_0, \dots, k_{J-1}} w_{k_0 \dots k_{J-1}}^* \nu_{k_0 \dots k_{J-1}}$$

where $\nu_{k_0 \dots k_{J-1}}$ is the Gaussian barycenter for W_2 between the components $\mu_0^{k_0}, \dots, \mu_{J-1}^{k_{J-1}}$, and w^* is the optimal solution of (6.3). Moreover, this barycenter has less than $K_0 + \dots + K_{J-1} - J + 1$ non-zero coefficients.

Proof. This follows directly from the proof of the previous propositions. The linear program (6.3) has $K_0 + \dots + K_{J-1} - J + 1$ affine constraints, and thus must have at least a solution with less than $K_0 + \dots + K_{J-1} - J + 1$ components. \blacksquare

To conclude this section, it is important to emphasize that the problem of barycenters for the distance GW_2 , as defined in (6.8), is completely different from

$$(6.8) \quad \inf_{\nu \in GMM_d(\infty)} \sum_{j=0}^{J-1} \lambda_j W_2^2(\mu_j, \nu).$$

Indeed, since $GMM_d(\infty)$ is dense in $\mathcal{P}_2(\mathbb{R}^d)$ and the total cost on the right is continuous on $\mathcal{P}_2(\mathbb{R}^d)$, the infimum in (6.8) is exactly the same as the infimum over $\mathcal{P}_2(\mathbb{R}^d)$. Even if the barycenter for W_2 is not a mixture itself, it can be approximated by a sequence of Gaussian mixtures with any desired precision. Of course, these mixtures might have a very high number of components in practice.

6.3. Some examples. The previous propositions give us a very simple way to compute barycenters between Gaussian mixtures for the metric GW_2 . For given mixtures μ_0, \dots, μ_{J-1} , we first compute all the values $MW_2(\mu_0^{k_0}, \dots, \mu_{J-1}^{k_{J-1}})$ between their components (and these values can be computed iteratively, see Section 2.5.2) and the corresponding Gaussian barycenters $\nu_{k_0 \dots k_{J-1}}$. Then we solve the linear program (6.3) to find w^* .

Figure 4 shows the barycenters between the following simple two dimensional mixtures

$$\begin{aligned} \mu_0 &= \frac{1}{3} \mathcal{N} \left(\begin{pmatrix} 0.5 \\ 0.75 \end{pmatrix}, 0.025 \begin{pmatrix} 0.1 & 0 \\ 0 & 0.05 \end{pmatrix} \right) + \frac{1}{3} \mathcal{N} \left(\begin{pmatrix} 0.5 \\ 0.25 \end{pmatrix}, 0.025 \begin{pmatrix} 0.1 & 0 \\ 0 & 0.05 \end{pmatrix} \right) \\ &\quad + \frac{1}{3} \mathcal{N} \left(\begin{pmatrix} 0.5 \\ 0.5 \end{pmatrix}, 0.025 \begin{pmatrix} 0.06 & 0 \\ 0.05 & 0.05 \end{pmatrix} \right), \\ \mu_1 &= \frac{1}{4} \mathcal{N} \left(\begin{pmatrix} 0.25 \\ 0.25 \end{pmatrix}, 0.01 I_2 \right) + \frac{1}{4} \mathcal{N} \left(\begin{pmatrix} 0.75 \\ 0.75 \end{pmatrix}, 0.01 I_2 \right) + \frac{1}{4} \mathcal{N} \left(\begin{pmatrix} 0.7 \\ 0.25 \end{pmatrix}, 0.01 I_2 \right) \\ &\quad + \frac{1}{4} \mathcal{N} \left(\begin{pmatrix} 0.25 \\ 0.75 \end{pmatrix}, 0.01 I_2 \right), \\ \mu_2 &= \frac{1}{4} \mathcal{N} \left(\begin{pmatrix} 0.5 \\ 0.75 \end{pmatrix}, 0.025 \begin{pmatrix} 1 & 0 \\ 0 & 0.05 \end{pmatrix} \right) + \frac{1}{4} \mathcal{N} \left(\begin{pmatrix} 0.5 \\ 0.25 \end{pmatrix}, 0.025 \begin{pmatrix} 1 & 0 \\ 0 & 0.05 \end{pmatrix} \right) \\ &\quad + \frac{1}{4} \mathcal{N} \left(\begin{pmatrix} 0.25 \\ 0.5 \end{pmatrix}, 0.025 \begin{pmatrix} 0.05 & 0 \\ 0 & 1 \end{pmatrix} \right) + \frac{1}{4} \mathcal{N} \left(\begin{pmatrix} 0.75 \\ 0.5 \end{pmatrix}, 0.025 \begin{pmatrix} 0.05 & 0 \\ 0 & 1 \end{pmatrix} \right), \\ \mu_3 &= \frac{1}{3} \mathcal{N} \left(\begin{pmatrix} 0.8 \\ 0.7 \end{pmatrix}, 0.01 \begin{pmatrix} 2 & 0 \\ 1 & 1 \end{pmatrix} \right) + \frac{1}{3} \mathcal{N} \left(\begin{pmatrix} 0.2 \\ 0.7 \end{pmatrix}, 0.01 \begin{pmatrix} 2 & 0 \\ -1 & 1 \end{pmatrix} \right) \\ &\quad + \frac{1}{3} \mathcal{N} \left(\begin{pmatrix} 0.5 \\ 0.3 \end{pmatrix}, 0.01 \begin{pmatrix} 6 & 0 \\ 0 & 1 \end{pmatrix} \right), \end{aligned}$$

where I_2 is the 2×2 identity matrix. Each barycenter is a mixture of at most $K_0 + K_1 + K_2 + K_3 - 4 + 1 = 11$ components. By thresholding the mixtures densities, this yields barycenters between 2-D shapes.

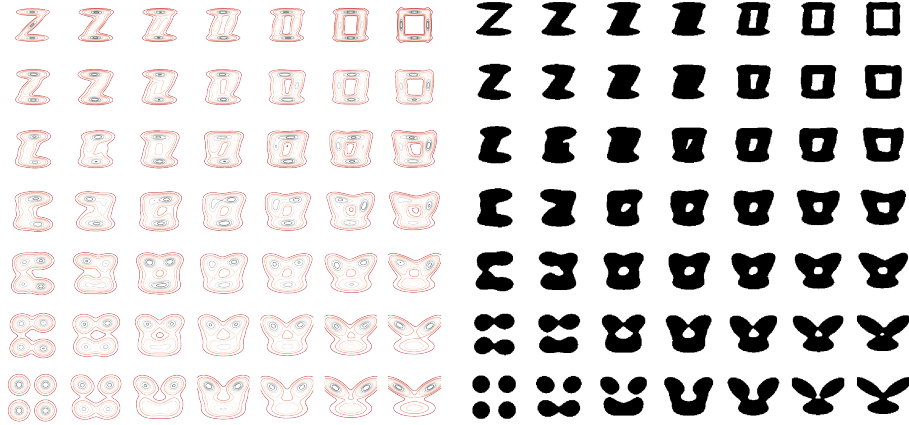


Figure 4. GW_2 -barycenters between 4 Gaussian mixtures μ_0, μ_1, μ_2 and μ_3 . On the left, some level sets of the distributions are displayed. On the right, densities thresholded at level 1 are displayed. We use bilinear weights with respect to the four corners of the square.

To go further, Figure 5 shows barycenters where more involved shapes have been approxi-

mated by mixtures of 12 Gaussian components each. Observe that, even if some of the original shapes (the star, the cross) have symmetries, these symmetries are not necessarily respected by the estimated GMM, and thus not preserved in the barycenters. This could be easily solved by imposing some symmetry in the GMM estimation for these shapes.



Figure 5. Barycenters between four mixtures of 12 Gaussian components, $\mu_0, \mu_1, \mu_2, \mu_3$ for the metric GW_2 . The weights are bilinear with respect to the four corners of the square.

7. From the GMM optimal plan to an assignment. In many applications, we need not only to have the optimal transport plan but we need to have an assignment giving for each $x \in \mathbb{R}^d$ a corresponding value $T(x) \in \mathbb{R}^d$. Let μ_0 and μ_1 be two GMM. Then, the optimal transport plan between μ_0 and μ_1 for GW_2 is given by

$$\gamma(x, y) = \sum_{k,l} w_{k,l}^* g_{m_0^k, \Sigma_0^k}(x) \delta_{y=T_{k,l}(x)}.$$

It is not of the form $(\text{Id}, T) \# \mu_0$ (see also Figure 1 for an example), but we can however define a unique assignment of each x , for instance by setting

$$T_{\text{mean}}(x) = \mathbb{E}_\gamma(Y|X = x),$$

where here (X, Y) is distributed according to the probability distribution γ . Then, since the distribution of $Y|X = x$ is given by the discrete distribution

$$\sum_{k,l} p_{k,l}(x) \delta_{T_{k,l}(x)} \quad \text{with} \quad p_{k,l}(x) = \frac{w_{k,l}^* g_{m_0^k, \Sigma_0^k}(x)}{\sum_j \pi_0^j g_{m_0^j, \Sigma_0^j}(x)},$$

we get that

$$T_{mean}(x) = \frac{\sum_{k,l} w_{k,l}^* g_{m_0^k, \Sigma_0^k}(x) T_{k,l}(x)}{\sum_k \pi_0^k g_{m_0^k, \Sigma_0^k}(x)}.$$

Notice that the T_{mean} defined this way is an assignment that will not necessarily satisfy the properties of an optimal transport map. In particular, in dimension $d = 1$, the map T_{mean} may not be increasing: each $T_{k,l}$ is increasing but because of the weights that depend on x , their weighted sum is not necessarily increasing. Another issue is that $T_{mean} \# \mu_0$ may be “far” from the target distribution μ_1 . This happens for instance, in 1D, when $\mu_0 = \mathcal{N}(0, 1)$ and μ_1 is the mixture of $\mathcal{N}(-a, 1)$ and $\mathcal{N}(a, 1)$, each with weight 0.5. In this extreme case we even have that T_{mean} is the identity map, and thus $T_{mean} \# \mu_0 = \mu_0$, that can be very far from μ_1 when a is large.

Now, another way to define an assignment is to define it as a random assignment using the optimal plan γ . More precisely we can define

$$T_{rand}(x) = T_{k,l}(x) \quad \text{with probability} \quad p_{k,l}(x) = \frac{w_{k,l}^* g_{m_0^k, \Sigma_0^k}(x)}{\sum_j \pi_0^j g_{m_0^j, \Sigma_0^j}(x)}.$$

An example of the results obtained with such a random assignment is shown on Figure 7. Notice that the final transported distribution $T_{rand} \# \mu_0$ is much closer to the target distribution μ_1 than with T_{mean} .

8. Two applications in image processing. We have already illustrated the behaviour of the distance GW_2 in small dimension. In the following, we investigate more involved examples in larger dimension. In the last ten years, optimal transport has been thoroughly used for various applications in image processing and computer vision, including color transfer, texture synthesis, shape matching. We focus here on two simple applications: on the one hand, color transfer, that involves to transport mass in dimension $d = 3$ since color histograms are 3D histograms, and on the other hand patch-based texture synthesis, that necessitates transport in dimension p^2 for $p \times p$ patches. These two applications require to compute transport plans or barycenters between potentially millions of points. We will see that the use of GW_2 makes these computations much easier and faster than the use of classical optimal transport, while yielding excellent visual results.

8.1. Color transfer. We start with the problem of color transfer. A discrete color image can be seen as a function $u : \Omega \rightarrow \mathbb{R}^3$ where $\Omega = \{0, \dots, n_r - 1\} \times \{0, \dots, n_c - 1\}$ is a discrete grid. The image size is $n_r \times n_c$ and for each $i \in \Omega$, $u(i) \in \mathbb{R}^3$ is a set of three values corresponding to the intensities of red, green and blue in the color of the pixel. Given two images u_0 and u_1 on grids Ω_0 and Ω_1 , we define the discrete color distributions $\eta_k = \frac{1}{|\Omega_k|} \sum_{i \in \Omega_k} \delta_{u_k(i)}$, $k = 0, 1$,

and we approximate these two distributions by Gaussian mixtures μ_0 and μ_1 thanks to the Expectation-Maximization (EM) algorithm³. Keeping the notations used previously in the paper, we write K_k the number of Gaussian components in the mixture μ_k , for $k = 0, 1$. We compute the GW_2 map between these two mixtures and the corresponding T_{mean} . We use it to compute $T_{mean}(u_0)$, an image with the same content as u_0 but with colors much closer to those of u_1 . Figure 6 illustrates this process on two paintings by Renoir and Gauguin, respectively *Le déjeuner des canotiers* and *Manhana no atua*. For this experiment, we choose $K_0 = K_1 = 10$. The corresponding transport map for GW_2 is relatively fast to compute (less than one minute with a non-optimized Python implementation, using the POT library [10] for computing the map between the discrete distributions of 10 masses). We also show on the same figure $T_{rand}(u_0)$ and the result of the sliced optimal transport [17, 4], since the complete optimal transport on such huge discrete distributions (approximately 800000 Dirac masses for these 1024×768 images) is hardly tractable in practice. As could be expected, the image $T_{rand}(u_0)$ is much noisier than the image $T_{mean}(u_0)$. We show on Figure 7 the discrete color distributions of these different images and the corresponding classes provided by EM (each point is assigned to its most likely class).

We show on the last line of Figure 6 the color transfer result with only $K_0 = K_1 = 3$ classes in each mixture. As we can see, the color distribution of $T_{mean}(u_0)$ in this case is too far from the one of u_1 and the approximation by the mixtures is probably too rough to represent the complexity of the color data properly. On the contrary, we have observed that increasing the number of components does not necessarily help since the corresponding transport map will lose regularity. For color transfer experiments, we found in practice that using around 10 components yields the best results.

Color transfer is very often used as a last step of texture synthesis experiments. In the recent neural network approach by Gatys et al. [13] for instance, this color transfer is applied separately on the three dimensions of the color distributions. Figure 8 shows the result of this separable optimal transport on a texture synthesis example. This solution, while not satisfying, is often used in the literature as a fast and simple way to transfer color between images. It often results in color artifacts which are not present in $T_{mean}(u_0)$.

We end this section with a color manipulation experiment, shown on Figure 9. Four different images being given, we create barycenters for GW_2 between their four color palettes (represented again by mixtures of 10 Gaussian components), and we modify the first of the four images so that its color palette spans this space of barycenters. For this experiment (and this experiment only), a spatial regularization step is applied in post-processing [16] to remove some artifacts created by these color transformations between highly different images.

8.2. Texture synthesis. Given an exemplar texture image $u : \Omega \rightarrow R^3$, the goal of texture synthesis is to synthesize images with the same perceptual characteristics as u , while keeping some innovative content. The literature on texture synthesis is rich, and we will only focus here on a bilevel approach proposed recently in [11]. The method relies on the optimal transport between a continuous (Gaussian or Gaussian mixtures) distribution and a discrete distribution (distribution of the patches of the exemplar texture image). The first step of the method can be described as follows. For a given exemplar image $u : \Omega \rightarrow R^3$, the authors compute the

³In practice, we use the *scikit-learn* implementation of EM with the *kmeans* initialization.



Figure 6. First line, images u_0 and u_1 (two paintings by Renoir and Gauguin). Second line, $T_{\text{mean}}(u_0)$ and $T_{\text{rand}}(u_0)$. Third line, color transfer with the sliced optimal transport [17, 4], that we denote by $SOT(u_0)$ and result of GW_2 transport with only 3 Gaussian components for each mixture.

asymptotic discrete spot noise (ADSN) associated with u , which is the stationary Gaussian random field $U : \mathbb{Z}^2 \rightarrow \mathbb{R}^3$ with same mean and covariance as u , *i.e.*

$$\forall x \in \mathbb{Z}^2, U(x) = \bar{u} + \sum_{y \in \mathbb{Z}^2} t_u(y) W(x - y), \quad \text{where} \quad \begin{cases} \bar{u} = \frac{1}{|\Omega|} \sum_{x \in \Omega} u(x) \\ t_u = \frac{1}{\sqrt{|\Omega|}} (u - \bar{u}) \mathbf{1}_\Omega, \end{cases}$$

with W a standard normal Gaussian white noise on \mathbb{Z}^2 . Once the ADSN U is computed, they extract the set S of all $p \times p$ sub-images (also called *patches*) of u . They define η_1 the empirical distribution of this set of patches (thus η_1 is in dimension $3 \times p \times p$, *i.e.* 27 for $p = 3$) and η_0 the Gaussian distribution of patches of U , and compute the semi-discrete optimal transport

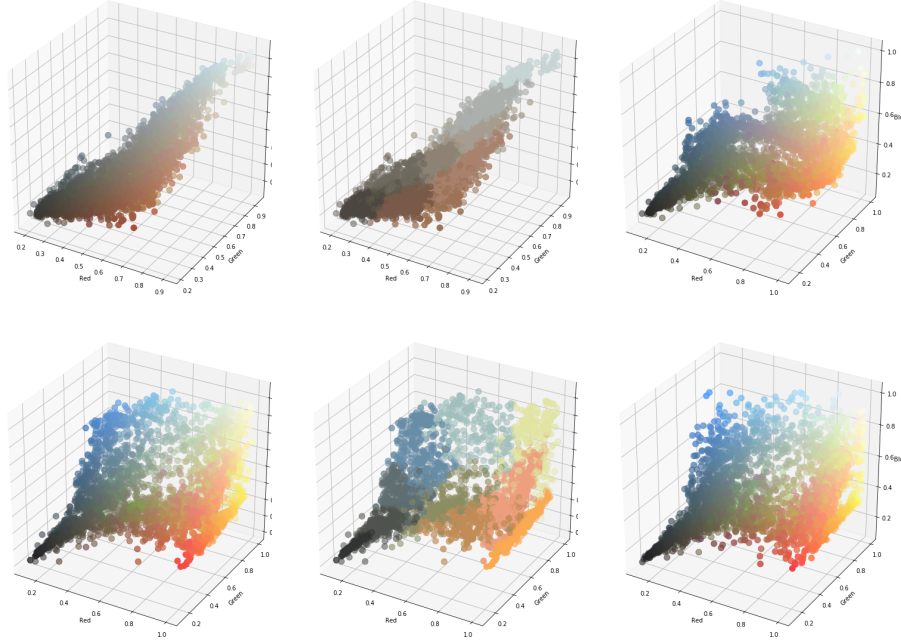


Figure 7. The images u_0 and u_1 are the ones of Figure 6. First line: color distribution of the image u_0 , the 10 classes found by the EM algorithm, and color distribution of $T_{mean}(u_0)$. Second line: color distribution of the image u_1 , the 10 classes found by the EM algorithm, and color distribution of $T_{rand}(u_0)$.

map T_{SD} from η_0 to η_1 . This map T_{SD} is then applied to each patch of a realization of U , and an output synthesized image v is obtained by averaging the transported patches at each pixel. Since the semi-discrete optimal transport step is numerically very expensive in such high dimension, we propose to make use of the GW_2 distance instead. For that, we approximate the two discrete patch distributions of u and U by Gaussian Mixture models μ_0 and μ_1 , and we compute the optimal map T_{mean} for GW_2 between them. The rest of the algorithm is similar to the one described in [11]. In practice, we use $K_0 = K_1 = 10$, as in color transfer, and 3×3 color patches. Figure 10 shows the results for different choices of exemplar images u .

9. Discussion and conclusion. In this paper, we have defined a Wasserstein-type distance on the set of Gaussian mixture models, by restricting the set of possible coupling measures to Gaussian mixtures. We have shown that this distance, with an explicit discrete formulation, is easy to compute and suitable to compute transport plans or barycenters in high dimensional problems where the classical Wasserstein distance remains difficult to handle. Observe that the distance GW_2 could be extended to other types of mixtures, as soon as we have an identifiability property similar to the one used in the proof of Proposition 4. In practice, Gaussian mixture models are versatile enough to represent large classes of concrete and applied problems. One important question raised by the introduced framework is how to estimate the mixtures for discrete data, since the result obtained will depend on the number of Gaussian components in the mixtures and on the inference of their parameters. If the number of

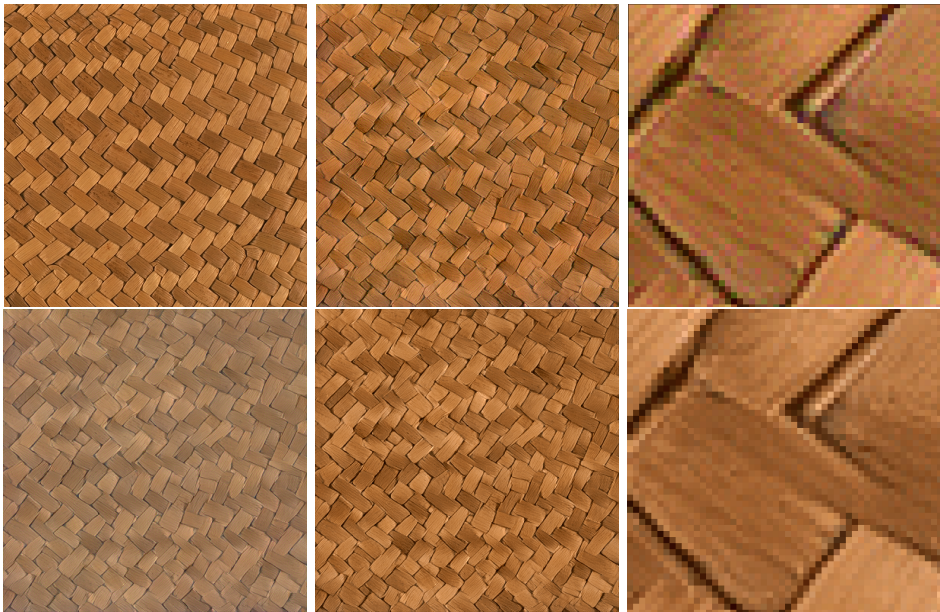


Figure 8. First column: a texture u_0 (top) and its corresponding synthesis u_1 by the neural network method [13]. Second column: the color palette of u_1 is transferred so that it matches the one of u_0 . Top: separable color transfer. Bottom: color transfer in 3D for GW_2 , each palette being represented by a mixture of 10 Gaussians. Last column: zooms on the results of column 2. Observe the color artifacts created by the separable optimal transport.

Gaussian components is chosen large enough, and covariances small enough, the transport plan for GW_2 will look very similar to the one of W_2 , but at the price of a high computational cost. If, on the contrary, we choose a very small number of components (like in the color transfer experiments of Section 8.1), the resulting optimal transport map will be much simpler, which seems to be desirable for some applications.

REFERENCES

- [1] M. AGUEH AND G. CARLIER, *Barycenters in the Wasserstein space*, SIAM Journal on Mathematical Analysis, 43 (2011), pp. 904–924.
- [2] P. C. ÁLVAREZ-ESTEBAN, E. DEL BARRIO, J. CUESTA-ALBERTOS, AND C. MATRÁN, *A fixed-point approach to barycenters in Wasserstein space*, Journal of Mathematical Analysis and Applications, 441 (2016), pp. 744–762.
- [3] J. BION-NADAL AND D. TALAY, *On a Wasserstein-type distance between solutions to stochastic differential equations*, Ann. Appl. Probab., 29 (2019), pp. 1609–1639, <https://doi.org/10.1214/18-AAP1423>.
- [4] N. BONNEEL, J. RABIN, G. PEYRÉ, AND H. PFISTER, *Sliced and Radon Wasserstein barycenters of measures*, Journal of Mathematical Imaging and Vision, 51 (2015), pp. 22–45.
- [5] Y. CHEN, T. T. GEORGIU, AND A. TANNENBAUM, *Optimal Transport for Gaussian Mixture Models*, IEEE Access, 7 (2019), pp. 6269–6278, <https://doi.org/10.1109/ACCESS.2018.2889838>.
- [6] Y. CHEN, J. YE, AND J. LI, *Aggregated Wasserstein Distance and State Registration for Hidden Markov Models*, IEEE Transactions on Pattern Analysis and Machine Intelligence, (2019), <https://doi.org/10.1109/TPAMI.2019.2908635>.
- [7] J. DELON AND A. HOUDARD, *Gaussian priors for image denoising*, in Denoising of Photographic Images



Figure 9. In this experiment, the top left image is modified in such a way that its color palette goes through the GW_2 -barycenters between the color palettes of the four corner images. Each color palette is represented as a mixture of 10 Gaussian components. The weights used for the barycenters are bilinear with respect to the four corners of the rectangle.

- and Video, Springer, 2018, pp. 125–149.
- [8] A. P. DEMPSTER, N. M. LAIRD, AND D. B. RUBIN, *Maximum likelihood from incomplete data via the EM algorithm*, Journal of the Royal Statistical Society: Series B (Methodological), 39 (1977), pp. 1–22.
 - [9] D. DOWSON AND B. LANDAU, *The Fréchet distance between multivariate normal distributions*, Journal of multivariate analysis, 12 (1982), pp. 450–455.
 - [10] R. FLAMARY AND N. COURTY, *POT Python Optimal Transport library*, 2017, <https://github.com/rflamary/POT>.
 - [11] B. GALERNE, A. LECLAIRE, AND J. RABIN, *Semi-discrete optimal transport in patch space for enriching Gaussian textures*, in International Conference on Geometric Science of Information, Springer, 2017, pp. 100–108.
 - [12] W. GANGBO AND A. ŚWIKECH, *Optimal maps for the multidimensional Monge-Kantorovich problem*, Communications on Pure and Applied Mathematics: A Journal Issued by the Courant Institute of Mathematical Sciences, 51 (1998), pp. 23–45.
 - [13] L. A. GATYS, A. S. ECKER, AND M. BETHGE, *Texture synthesis using convolutional neural networks*, in NIPS, 2015.
 - [14] A. HOUDARD, C. BOUVEYRON, AND J. DELON, *High-dimensional mixture models for unsupervised image denoising (HDMM)*, SIAM Journal on Imaging Sciences, 11 (2018), pp. 2815–2846.
 - [15] G. PEYRÉ AND M. CUTURI, *Computational optimal transport*, Foundations and Trends® in Machine Learning, 11 (2019), pp. 355–607.
 - [16] J. RABIN, J. DELON, AND Y. GOUSSEAU, *Removing artefacts from color and contrast modifications*, IEEE Transactions on Image Processing, 20 (2011), pp. 3073–3085.
 - [17] J. RABIN, G. PEYRÉ, J. DELON, AND M. BERNOT, *Wasserstein barycenter and its application to texture*

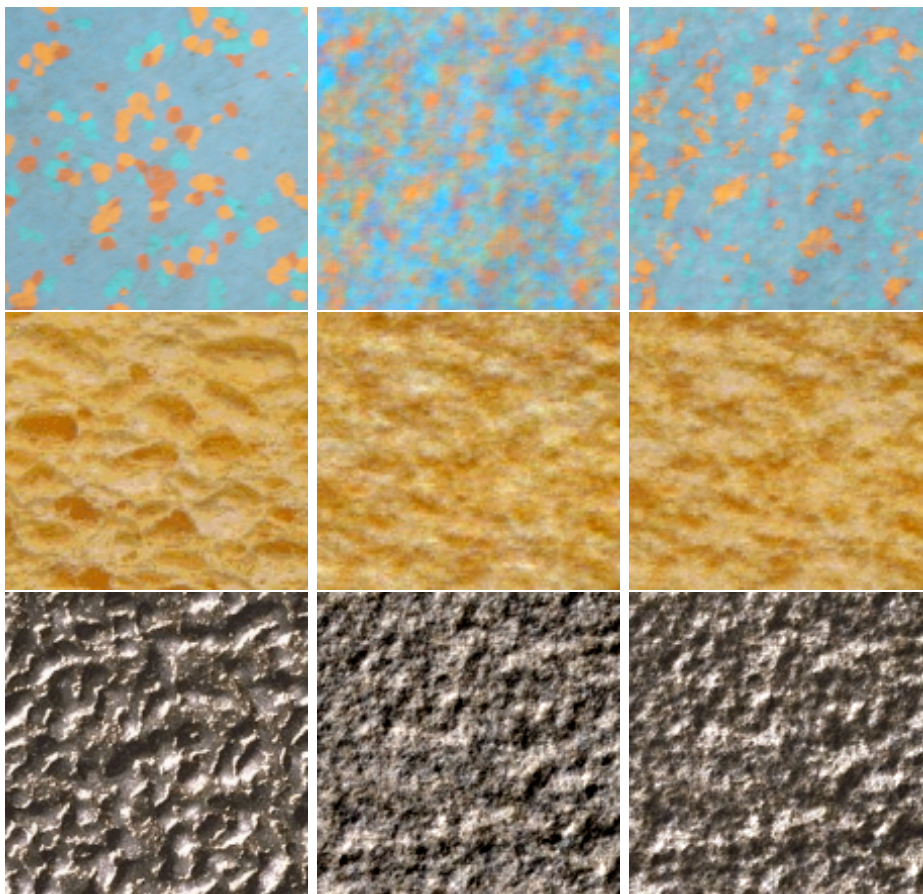


Figure 10. Left, original texture u . Middle, ADSN U . Right, synthesized version.

- mixing*, in International Conference on Scale Space and Variational Methods in Computer Vision, Springer, 2011, pp. 435–446.
- [18] L. RÜSCHENDORF AND L. UCKELMANN, *On the n -coupling problem*, Journal of multivariate analysis, 81 (2002), pp. 242–258.
- [19] F. SANTAMBROGIO, *Optimal Transport for Applied Mathematicians*, Birkäuser, Basel, 2015.
- [20] A. M. TEODORO, M. S. ALMEIDA, AND M. A. FIGUEIREDO, *Single-frame Image Denoising and Inpainting Using Gaussian Mixtures*, in ICPRAM (2), 2015, pp. 283–288.
- [21] C. VILLANI, *Topics in Optimal Transportation Theory*, vol. 58 of Graduate Studies in Mathematics, American Mathematical Society, 2003.
- [22] C. VILLANI, *Optimal transport: old and new*, vol. 338, Springer Science & Business Media, 2008.
- [23] Y.-Q. WANG AND J.-M. MOREL, *SURE Guided Gaussian Mixture Image Denoising*, SIAM Journal on Imaging Sciences, 6 (2013), pp. 999–1034, <https://doi.org/10.1137/120901131>.
- [24] G.-S. XIA, S. FERRADANS, G. PEYRÉ, AND J.-F. AUJOL, *Synthesizing and mixing stationary Gaussian texture models*, SIAM Journal on Imaging Sciences, 7 (2014), pp. 476–508.
- [25] S. J. YAKOWITZ AND J. D. SPRAGINS, *On the identifiability of finite mixtures*, Ann. Math. Statist., 39 (1968), pp. 209–214, <https://doi.org/10.1214/aoms/1177698520>.
- [26] G. YU, G. SAPIRO, AND S. MALLAT, *Solving inverse problems with piecewise linear estimators: from Gaussian mixture models to structured sparsity*, IEEE Trans. Image Process., 21 (2012), pp. 2481–99, <https://doi.org/10.1109/TIP.2011.2176743>.

- [27] D. ZORAN AND Y. WEISS, *From learning models of natural image patches to whole image restoration*, in 2011 Int. Conf. Comput. Vis., IEEE, Nov. 2011, pp. 479–486, <https://doi.org/10.1109/ICCV.2011.6126278>.